Universiteit Utrecht

Heavy metal contamination in the Geul River:

Assessment of the metal inventory in and export from the river valley.

Utrecht University

Faculty of Geosciences.

Department of Earth Sciences.

MSc Thesis Hydrology.

Supervisors:

Dr. M. v.d. Perk

Dr. H. Middelkoop

Laura Miguel Ayala

3439216

29th July, 2011.

Summary

One of the most important environmental problems in many fluvial systems is that of heavy metal contamination. Metal mining has caused spreading and accumulation of heavy metals in many river basins during the last century. As it has been discussed in previous studies (Dennis et al., 2008) floodplains can act as a metal storage for hundreds or thousands of years and become a source of heavy metals during floods.

Meandering rivers, such as the Geul River, are very dynamic systems where erosion and deposition processes can produce remobilization and redistribution of heavy metals over the catchment altering the quality of the water and disturbing the flora and fauna of the area.

Soil sample collection in the Dutch part of the Geul catchment was carried out during this project with the purpose of studying the distribution of zinc and lead within the Geul catchment. A total of nine cross-sections were performed in the upstream direction with a 4 km interval. The analysis of the samples was performed using a hand-held X-Ray fluorescence spectrometer (Thermo Fisher Scientific Niton® XL3t-600 hand-held XRF analyzer) and the results were statistically analysed. The statistical analysis of the samples shows a decrease in heavy metal content in the downstream direction. A general decrease in zinc and lead content was also found when the distance from the river increases. Results of the statistical analysis show by higher significance that downstream distance from the pollution source is a useful variable to explain the distribution of the heavy metals along the Geul catchment.

This study aimed to assess the annual export of zinc and lead from the Geul floodplain obtained after a one year simulation using the CAESAR model. These calculations were based on the average values of zinc and lead provided by the analysis of the samples previously mentioned together with the sediment results after a one year simulation of the CAESAR model. The assessed amounts of lead and zinc deposition for the year 2008 were 14.5 and 57.9 tons respectively. By comparing total and suspended sediment results of the model with other studies (Leenaers, 1989; De Moor, 2006) the results of the CAESAR model seem to be between 3-5 times higher. The reason for this can be that the model uses a 25 meter resolution, which makes the river wider than in reality and consequently more sediment is generated. Other irregularities in the Digital Elevation Map and the 'spin up' process where the model starts assuming uniform bed material over the whole catchment and generates high amounts of sediment during the first years of the simulation, can influence the final sediment results and therefore, the calculated amounts of zinc and lead can be overestimated.

Table of contents

Acknowledgements

I am thankful to Dr. M. v.d. Perk and Dr. H. Middelkoop for the supervision, suggestions and practical assistance during this study. I am grateful to CSO Consultance (Consultants for Environmental Management and Survey) for kindly providing the equipment to carry out the sample analysis, and especially to Björn Scheepers for his assistance and advice during this process. I gratefully acknowledge Tom Coulthard for allowing the use of CAESAR model during this study. I would like to thank Drs. Han Kessels and Ing. Peter Hulst (Waterschap Roer en Overmaas) for providing discharge and suspended sediment data for the Geul River and its tributaries. Furthermore, I wish to thank my family for their support and help, my colleagues and friends who contributed with their valuable comments and suggestions and in particular to Veronica Arribas Arcos for her collaboration during fieldwork.

1. Introduction

1.1 Problem definition

Heavy metal contamination of sediment within river systems is an important environmental problem in many fluvial systems around the world. Metal contaminated sediments have been historically released into river systems as a product of mining. Previous studies (Dennis et al., 2008) show that metals can remain stored in floodplains for hundreds or even thousands of years. Sediments work as large transporters of heavy metals enabling their interactions within the fluvial system. Older contaminated floodplain sediments continue to function as a major source of heavy metals during floods. Therefore, overbank sediments may be an important source of contaminated sediments.

Meandering rivers are very dynamic systems with high erosion and lateral migration rates. In these cases, remobilization of contaminants is an active process producing redistribution of heavy metals over the catchment. The presence of heavy metals in the river basin can alter the quality of the water and affect the flora and fauna of the area.

The Geul is a transboundary river that flows from the north-eastern part of Belgium into the Dutch province of Limburg, where it joins the Maas (Meuse) River. This river has been subject to the effects of human activities such as canalisation and heavy metal contamination due to mining activities in the Belgian part of the catchment which started during the 19th century. Heavy metal contamination (zinc, lead, cadmium and copper) can alter the high ecological value of this tributary of the Maas River.

1.2 Research objectives

The study area covers the part of the Geul catchment that is located in The Netherlands. The main purpose of this study is to investigate the distribution of heavy metals over the Geul River floodplain. The study focuses on zinc and lead. An extensive statistical analysis was carried out based on the data provided by the sample collection during the fieldwork performed for this study in order to examine the distribution of zinc and lead over the catchment.

Secondly, this study aims to assess the total amount of zinc and lead obtained after a one year simulation using the CAESAR model, by comparing the average values of zinc and lead found in the samples taken from the Geul catchment with the sediment results after the model simulation.

With the purpose of achieving these goals, this research aims to answer the following questions:

- What is the spatial variation of the heavy metals (zinc and lead) in the Geul floodplain?

- What is the total annual export of zinc and lead from the Geul floodplain according to a one year simulation with CAESAR model?

1.3 Research approach

This study has been carried out in accordance to an integrated approach based on specifically-collected data for this research project and results from modelling. Initially, a compilation of peer-reviewed studies was utilized to extract theoretical information that could be of use for this research (Chapters 1 and 2). Full references for all studies consulted are provided in the list of references. Sample collection and sample analysis (Chapter 3) were carried out in order to obtain the necessary data to perform an extensive data analysis which is presented in chapter 4. Furthermore, a modelling simulation was carried out in addition to sample analysis. The functioning of the model and its results are discussed in chapters 5 and 6. Lastly, a brief summary of the results from this research is presented in Chapter 7.

2. Study Area

2.1 Description of the area

The Geul River is a small meandering river which originates at the border between eastern Belgium and Germany. It flows through the southern part of the Netherlands (South-Limburg) into the Meuse River (Maas river in figure 1) located kilometers north from Maastricht. (De Moor and Verstraeten, 2008).

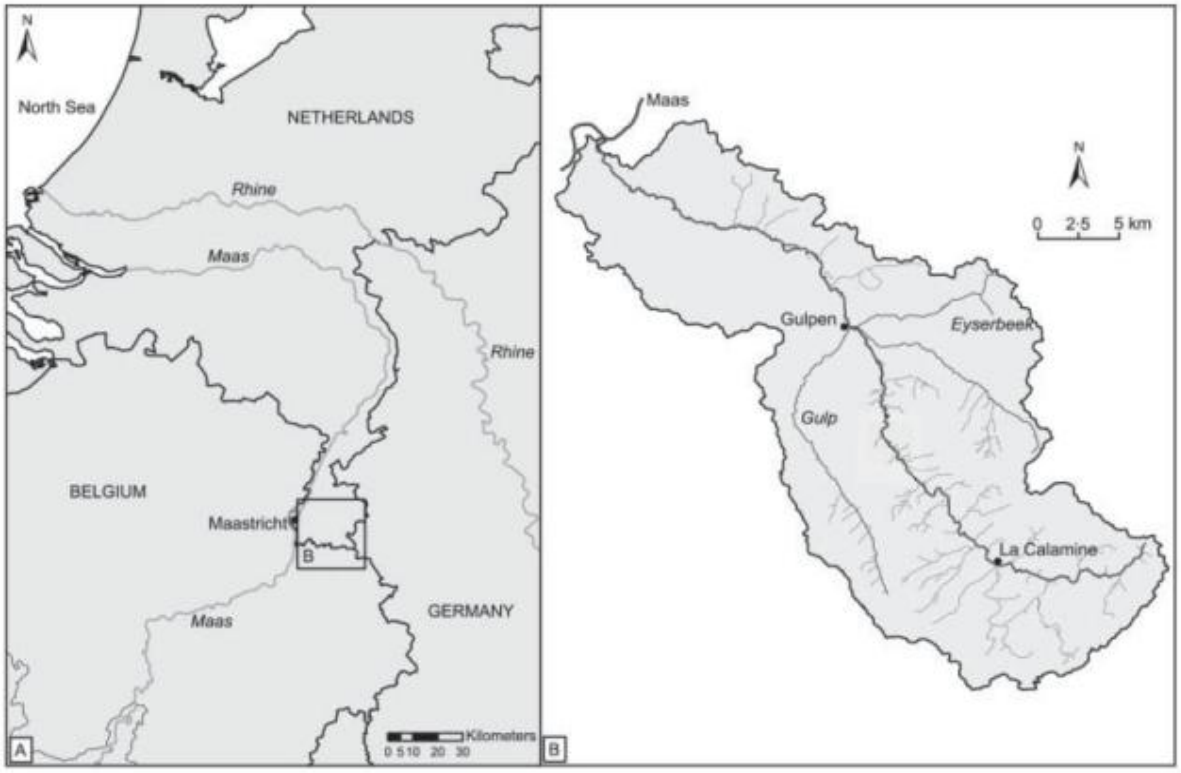

Figure 1. Location of the Geul River catchment (A) and a more detailed view of the study area (De Moor et al., 2007).

The Geul River catchment covers an area of 380 km². About 240 km² of the total area is located in The Netherlands. (De Moor and Verstraeten, 2008)

The total channel length is around 56 km, of which 36 km belong to The Netherlands and 22 km to Belgium (Leenaers, 1989). The altitude of the catchment varies from 50 to 400 m asl at the confluence with the Meuse River and in the headwaters respectively. The annual precipitation rate fluctuates within the range of 750 to 800 mm yr^{-1} in the area where the Geul joins the Meuse up to more than 1,000 mm yr^{-1} near the source area. (De Moor and Verstraeten, 2008).

The actual catchment of the Geul River can be described as large with irregular river valleys and flat plateaus that are locally and partly covered by alluvial fans. The floodplain is flat varying in

width from 200 m near the Belgian-Dutch border to 700 m near the union to the Meuse River. The Geul River is considered a fast flowing river with maximum lateral migration rates of 2 m yr^{-1}. (De Moor and Verstraeten, 2008).

The river channel width varies from 8 to more than 15 meters. The valley gradient varies within the range of 0.02 m m^{-1} to 0.0015 m m^{-1}. The average discharge is 3.4 m^3s^{-1} and fluctuates due to occasional peak discharges which can be larger than 40 m^3s^{-1}. Infrequent high peak discharges can be produce as a result of heavy thunderstorms. Events like this could cause local floods. (De Moor et al., 2007).

The geology of the river is characterized by Devonian and Carboniferous limestones, sandstones and shales in the Belgian and southern part of The Netherlands. Soils can be classified as silty loam Luvisols. (De Moor and Verstraeten, 2008).

The land use in the area is mainly farmland (pasture) and the landscape is mainly characterized by the presence of grassland in the river valley. Villages are situated on the hills of the valley as well as camp sites giving the Geul valley an important facet as a recreational area. (Leenaers, 1989). The Geul River is considered to be one of the few (partly) meandering rivers in The Netherlands. In the last decades, most of the rivers have been straightened and channelized, but due to the high ecological value of the Geul catchment local authorities allow its natural meandering. (De Moor et al., 2007).

2.2 Mining activities and metal dispersal

Many river catchments in the world have been influenced by mining processes that released metal contaminated sediments into their systems. The remobilization of these metals by erosion and deposition processes within the catchment can produce an important environmental impact on the fluvial system even long after the mining activities have been ended.

Studies in England carried out by Coulthard et al. (2003) have shown large longevity of heavy metal pollution in river sediments as more than 70% of the contaminants stay in the river system longer than 200 years. (Coulthard et Van de Wiel, 2011).

Mining activities have played an important role in the Geul basin during centuries. The main sites of mining and ore treatment are located in the Belgian part of the catchment. The most important mining centers were La Calamine, Plombières and Schamlgraf (figure 2). The exploitation of Zinc and Lead had its origin around the thirteenth century but it was during the nineteenth and twentieth centuries when the mining area started working on a commercial scale (Leenaers, 1989). Industrial operations started at La Calamine ore body in 1806 consisting mainly of zinc oxides. Industrial mining at Plombières and Schmalgraf began in 1844 and 1868 respectively dominating the Pb-Zn sulfides in both of them (Swennen et al., 1994). The last mine closed in 1938 but until 1950s the treatment of the metal ores continued (Leenaers, 1989). Due to the

inefficient techniques used and the dumping of tailings in large heaps, pollutants were released directly into the river and were accumulated in the river sediments.

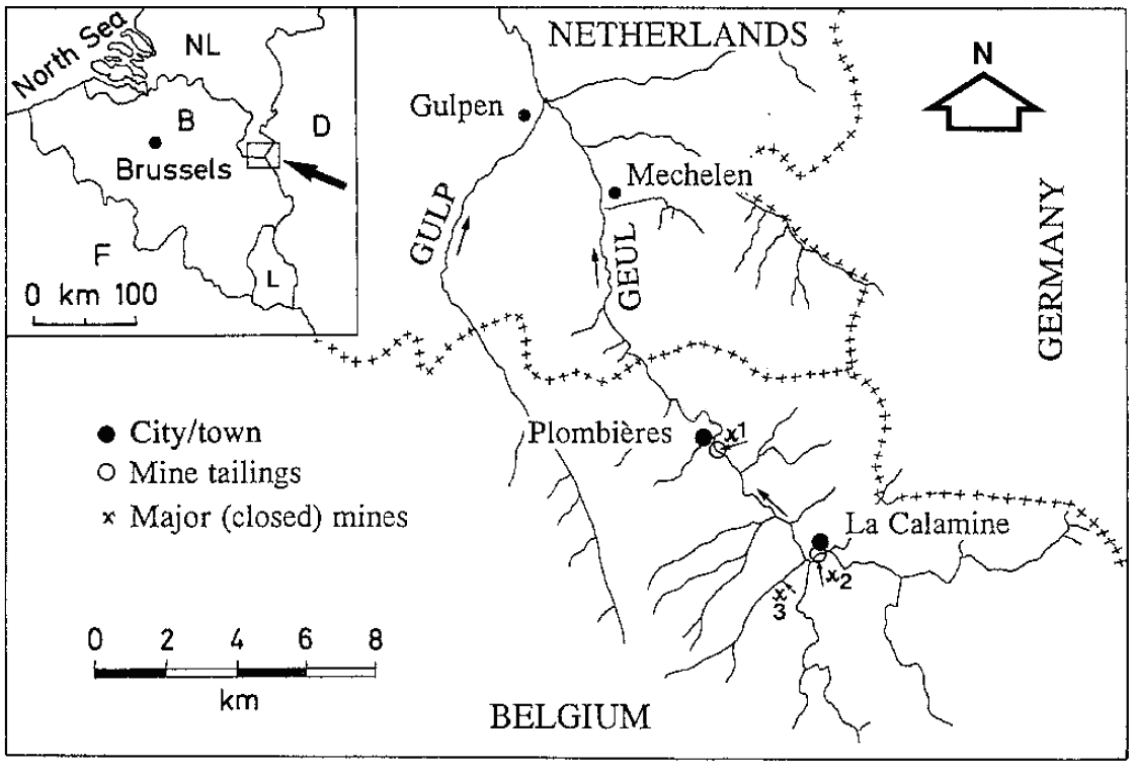

Figure 2. Location of the three mining centres: 1. Plombières; 2. La Calamine; 3 Schmalgraf (Swennen et al., 1994).

The years between 1845 and 1882 can be considered as the period where the peak of mining activities took place. The metals that were introduced into the river system originated from the mine water pumping and ore treatment effluent. This provided the river with high concentrations of suspended solids that made the river water more acid due to the oxidation of sulfides. As a result of this, the river water experienced a decrease in pH and an increase in its dissolved metal carrying capacity. (Stam, 1999).

The meandering character of the Geul River implies that processes such as erosion, transport and deposition play an important role in the downstream migration of sediments. This migration process can also be influenced by changes in the discharge of the river as for example peak discharges and consequent inundation of the floodplains. All these factors can influence the contents of heavy metals if the sediments of the Geul River.

The contamination of the sediments by zinc and lead has provided the necessary habitat conditions for the zinc flora (*Viola calaminaria*) to live in. It has been recently registered a decrease in the zinc flora populations. This could have partly been as a result of the meandering of the river as the lateral erosion produces dilution of the contaminated sediments. (De Moor et al., 2007).

Studies carried out by Dennis et al. (2008) consisting of fieldwork sampling to study sediment contamination in mined catchments found a gradual downstream reduction of contaminant concentrations. Hotspots of contamination can be found as a result of additional contaminant inputs from tributaries or by areas of preferential deposition as for example a widening of the valley in some areas. (Dennis et al., 2008).

As discussed by Dennis et al (2008), floodplains play an important role in the storage of metal-rich sediments. During overbank floods these sediments can be remobilized and re-deposited meaning that the frequency of flood events influences the remobilization-re-deposition rate. (Dennis et al., 2008).

In a study performed by Leenaers et al. (1989) in the Geul River decrease of metal concentrations on the downstream direction was also found. This is explained as a result of dilution processes with clean bed, bank and hillslope material. According to this study, discharge, distance to the source and floodplain geometry are important factors to consider when studying the metal dispersal in the catchment area. Results of this study show that suspended metal concentrations barely decrease with increasing discharge. This is because during high flood episodes the heavy metal sources have a greater activity than before. Total metal concentrations experience an exponential reduction with distance to the source by dilution processes. The geometry of the floodplain was found to have a large influence on the distribution of the pollutants at local scale. (Leenaers and Rang, 1989).

3. Methodology

3.1 Fieldwork and Sample collection

With the purpose of studying the metal dispersal in the Geul floodplain it was necessary to assess the heavy metal inventory over the Dutch part of the catchment. This was achieved through soil sample collection in the field along the river valley. Therefore, several locations were chosen over the catchment of the Geul River to perform the drillings. Nine cross-sections distributed approximately each 4 km in the upstream direction were performed.

The distribution of the drilling locations, numbered by transects along the river valley (figure 3), where given the following names:

1. Meerssen.
2. Strabeek.
3. Schin op Geul.
4. Keutenberg.
5. North Gulpen.
6. Partij.
7. Mechelen.
8. Terpoorten.
9. Cottessen.

In transect 3 (Schin op Geul), two locations were chosen (a and b) due to impossibility of performing the whole transect at location a as it was a private property. (Figure 3)

Coordinates of the exact locations of the transects can be found in Appendix 1.

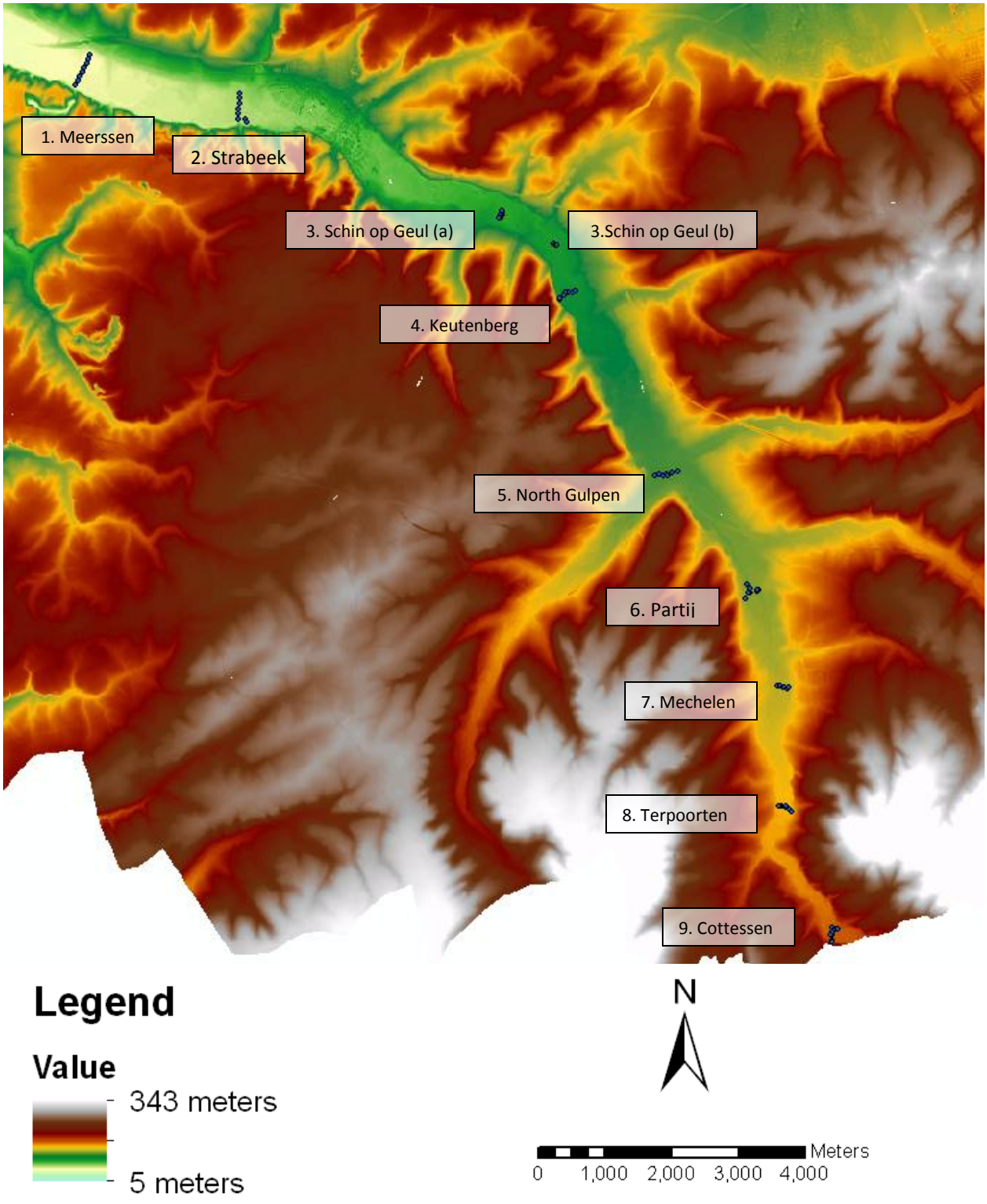

Figure 3. Drilling locations (nine transects) in the Geul catchment.

The cross-sections were done perpendicular to the direction of the valley. In each transect up to 11 corings were performed in each transect distributed in both sides of the river taking the width of the valley and the morphological units present in it into consideration. Soil samples were taken every 10 cm deep in each coring down to a maximum depth of 2.5 m. Total of some 1,238 samples were collected during this study. All samples were put in bags and labeled according to the sampling location and depth where they were taken from.

3.2 Sample analysis

The development of other techniques such as field portable X-ray fluorescence analyzers allows detecting and quantifying element concentrations in sediments in a fast, easy and accurate way. (Hürkamp et al., 2009).

With the purpose of assessing the heavy metal concentrations of the samples collected in the Geul floodplain CSO (Adviesbureau voor milieu, ruimte en water, Maastricht) kindly provided us with a hand-held X-Ray fluorescence spectrometer (Thermo Fisher Scientific Niton® XL3t-600 handheld XRF analyser) with which the measurements were performed (figure 4).

Figure 4. Thermo Fisher Scientific Niton® XL3t-600 handheld XRF analyser (LearnXRF, 2011).

This instrument allows analysis of trace elements based on the principles of X-Ray Fluorescense. The behaviour of atoms when they interact with radiation experiences some changes. When the X-rays (short wavelenght radiation) are applied to a sample of geological material, it becomes ionized. If the energy of the radiation is enough it can make an atom unstable. This means that an inner electron of the atom is disloged and an outer electron replaces its space. Consequently, there is some energy released from this new binding (as the binding with the outer electron implies less energy) which is called fluorescent radiation. (SERC, 2011).

The energy emitted when an electron moves from two different orbitals is characteristic of each particular element. Therefore, by assessing the energy emitted by a particular element, the identity of the element can be identified and in the same way its abundance can be quantified. (LearnXRF, 2011).

As it was mentioned before, the XRF analyzer can be brought to the field. Therefore, the heavy metal concentrations can be directly determined by in situ measurement. However, this instant measurement implies no pre-treatment of the sediment samples which might alter the quality of the measurement. (Hürkamp et al., 2009).

Studies carried out by Hürkamp et al. (2009) demonstrate that soil moisture content of the samples measured directly in the field leads to lower values of lead concentrations than the samples measured after being homogenized and dried in the laboratory. If the samples have more than 20% of water content the accuracy of the XRF analyzer measurements is no longer assured. (Hürkamp et al., 2009).

Therefore, the collected samples of the Geul floodplain were dried during two weeks at room temperature. Afterwards, they were manually homogenized using a mortar in order to obtain more representative average values of the locations where they were collected.

The XRF analysis was performed to assess the lead and zinc concentrations for every sample collected in the Geul valley. The XRF analyzer was previously calibrated at CSO. Measurement time was 60 seconds per sample. Blank measurements were carried out approximately every 17 samples. Measurements of cadmium were not carried out due to the large uncertainty of the obtained values from the XRF analyzer and the double time of measurement required for this element.

Due to the large number of samples and the restricted time to perform the analysis each sample was analyzed once. However, three samples per transect were randomly chosen to be analyzed five times each.

The samples were taken as it was previously explained from several vertical sections within 9 transects of the Geul valley. Therefore, the results of the XRF analysis provided with a catena of heavy metal concentration profiles of the soil (see section 4.1.1). Zinc and lead concentrations obtained by the XRF analysis were used to perform a statistical analysis (see section 4.2).

4. Spatial Pattern of Heavy metals in the Geul floodplain

4.1. Vertical soil profiles

Data obtained after measurements of the samples collected in transect 5 (North Gulpen) were chosen to show how lead and zinc concentrations are distributed along a vertical soil profile. The zinc and lead concentrations along vertical profiles (up to 1,7 meters deep) plotted on the following graphs (figures 5 to 11) are the resultant concentrations after having subtracted background values assumed for zinc (40 ppm) and lead (10 ppm). The vertical profiles of transects 1, 2, 3, 4, 6, 7, 8, and 9 can be found in Appendix 3.

4.1.1 Results

As a general pattern the following graphs (figures 5 to 11) show how vertical soil profiles experience a vertical decrease in lead and zinc concentrations. When comparing vertical zinc profiles (in pink) with lead profiles (in blue) within the same transect and coring it can be seen that peaks of higher concentration values occur at approximately the same depth.

However, zinc profiles indicate higher concentration values than the lead profiles. A remarkable increase in contamination can be observed above a depth of around 60 cm in most samples. In addition, an increase in heavy metal concentration can be observed below 90 cm that tends to decrease gradually.

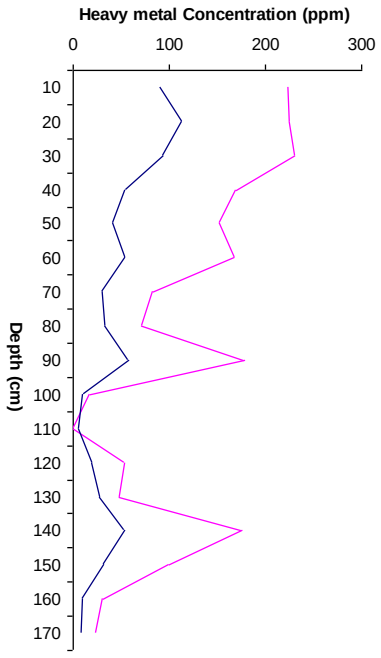

Figure 5. Metal concentration profile.

Transect 5 coring 1

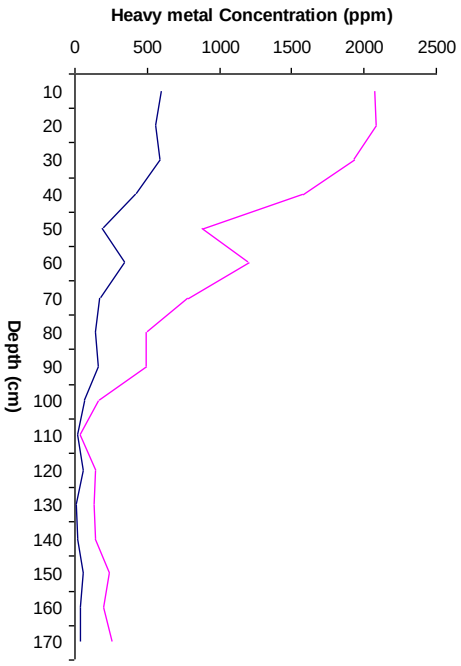

Figure 6. Metal concentration profile.

Transect 5 coring 2

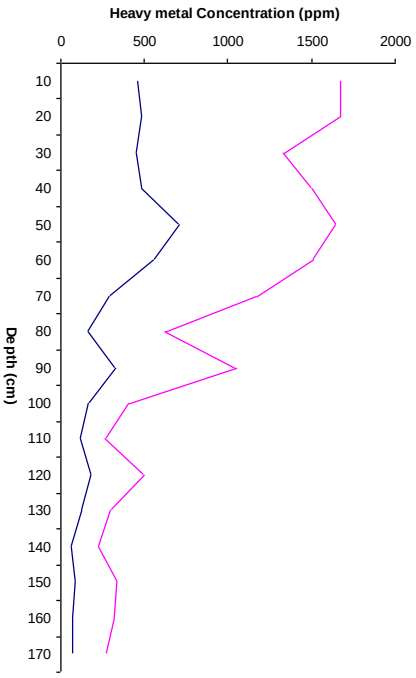

Figure 7. Metal concentration profile.

Transect 5 coring 3

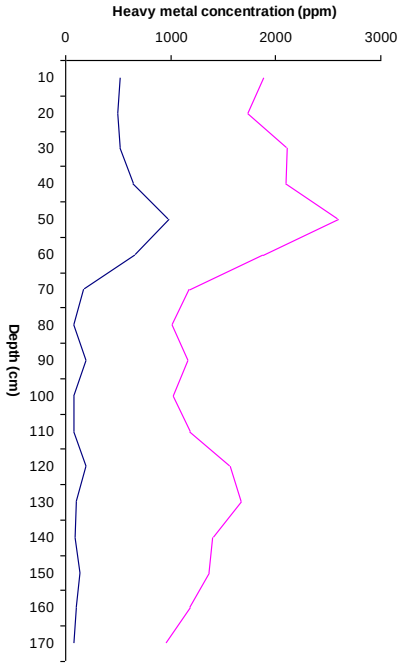

Figure 8. Metal concentration profile.

Transect 5 coring 4

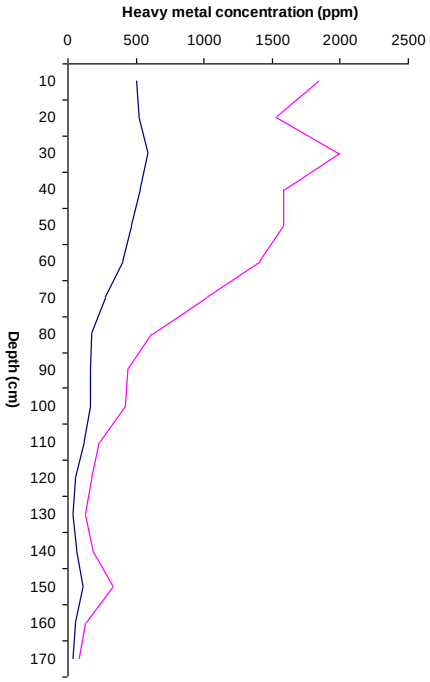

Figure 9. Metal concentration profile.

Transect 5 coring 5

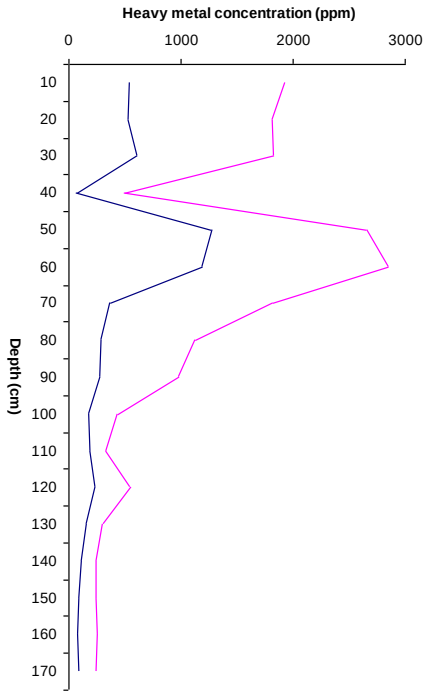

Figure 10. Metal concentration profile.

Transect 5 coring 6

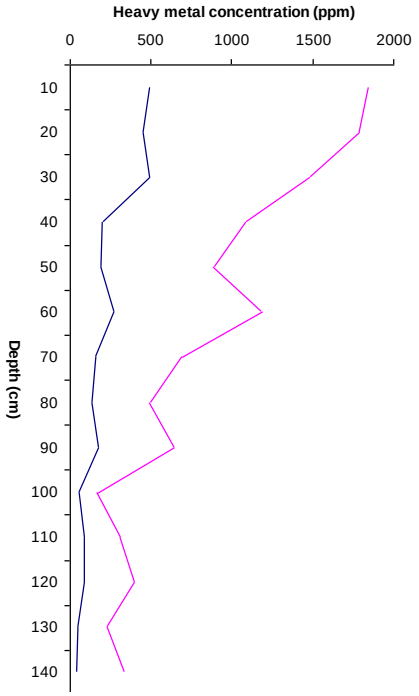

Figure 11. Metal concentration profile.

Transect 5 coring 7

4.1.2 Discussion

The heavy metal concentration profiles shown in the previous figures (figures 5 to 11) can be compared with other studies in the area such as the ones carried out by Swennen et al. (1994) and Stam (1999) as their results show a similar vertical pattern to the one obtained in the present study.

Swennen et al. (1994) analyzed three vertical profiles from a location approximately 1 km north of the mine tailings of Plombières. In general, they found lead to decrease gradually with depth while zinc experiences rather irregular behaviour with higher concentration peaks at around 100 cm deep. This increase in zinc content below a marked increase in lead content can be explained as a result of the earlier start of zinc mining operations at La Calamine in 1806. This ore body, which is the largest in the Geul catchment, consists nearly entirely of zinc-ore. (Swennen et al., 1994).

Soil profiles analyzed by Stam (1999) at a location approximately 12 km from the Duth-Belgian border also present an increase in zinc and lead metal content at 60 cm deep.

In the current study, higher zinc contents than lead contents are also found in the vertical profiles previously presented. This behaviour can be as well explained by the fact that zinc industrial mining started earlier than lead mining. As it was previously mentioned in section 2.2, zinc

industrial mining started at La Calamine in 1806 while lead and zinc industrial mining started at Plombières and Schmalgraf in 1844 and 1868 respectively.

It is important to mention that in some of the samples that belong to the deepest parts (deeper than 1.70 meters) of some corings, was observed a trend of increasing heavy metal concentration in the last and deepest layers. This anomalous behavior could be explained by historical artisanal mining activities dating back to the 14th century (Swennen et al., 1994). However, this is not the main research question in this study and therefore further investigation is needed.

4.2 Statistical Analysis of the data

4.2.1 Analysis of the precision of the data

This study is based upon a large dataset of samples. Errors in every dataset derived from the measurement equipment, human errors as for example during fieldwork or from any other source are inevitable.

Three samples of 7 transects (21 samples in total) were chosen to be analyzed five times each. One sample was taken from the shallowest part of the coring, one from the middle part and one from the deepest part in each of the 7 transects. Therefore, five values of lead and zinc concentrations were obtained for each selected sample. Thus as there are 5 lead and 5 zinc values for every 5 measurements of the same sample their average and standard deviation can be calculated.

The coefficient of variation (CV) was calculated to measure the variation within the heavy metal. The coefficient of variation by definition is a ratio between the standard deviation (SD) and the mean (X) (Bendel et al., 1989):

$$CV = SD / X$$

To graphically represent the uncertainty around the mean values, the standard error of the mean (SEM or SE if there is no ambiguity we are talking about the mean) was calculated (Altman and Bland, 2005). This was considered to be more appropriate statistics than standard deviation (SD) as SEM reflects the variability of the means, while SD refers to the variability of individual data points (Hassani et al., 2010).

Unlike the standard deviation, the standard error of the mean takes into account the sample size (N) by the following relation (Hassani et al., 2010):

$$SE = SD / \sqrt{N}$$

As the sample size is in the denominator, the larger N is the smaller SE will be. For the same reason, the smaller the variability of the data (SD) the smaller SE will be. The smaller the resultant SE the more accurate the mean of the data (Hassani et al., 2010).

- Results

The coefficient of variation was calculated for all the replicate samples, resulting in 8.2 % and 6.5 % for lead and zinc respectively.

The standard error of the mean for each five repeated samples was also calculated as it can be seen in the next graphs (Figures 12 and 13). The I bars represent the standard error values, where ± standard error value is added to the mean lead and zinc concentrations (ppm). The samples are named according to the following code: t8-1-030 corresponds to Transect 8-coring1-30 cm deep.

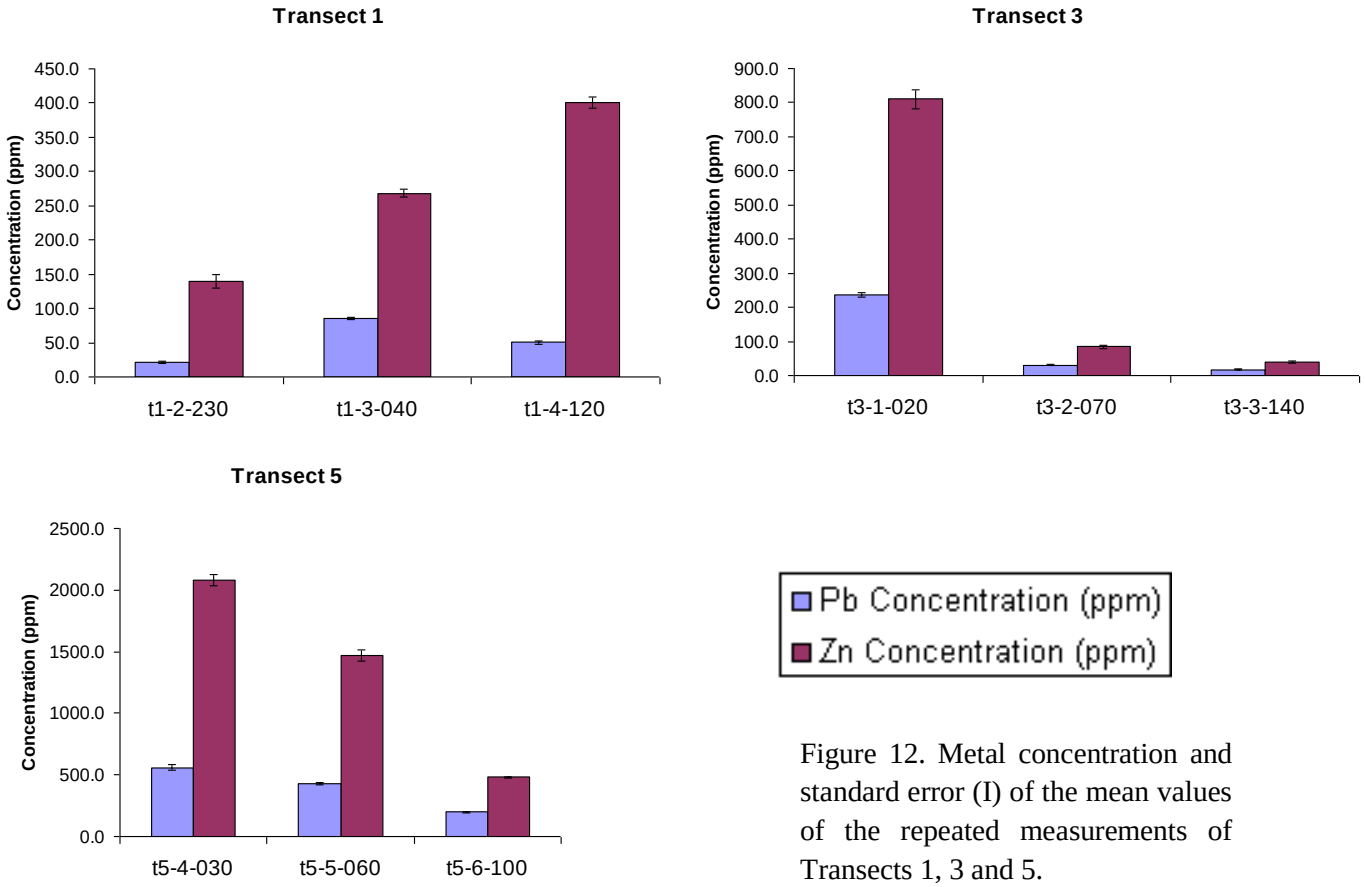

Figure 12. Metal concentration and standard error (I) of the mean values of the repeated measurements of Transects 1, 3 and 5.

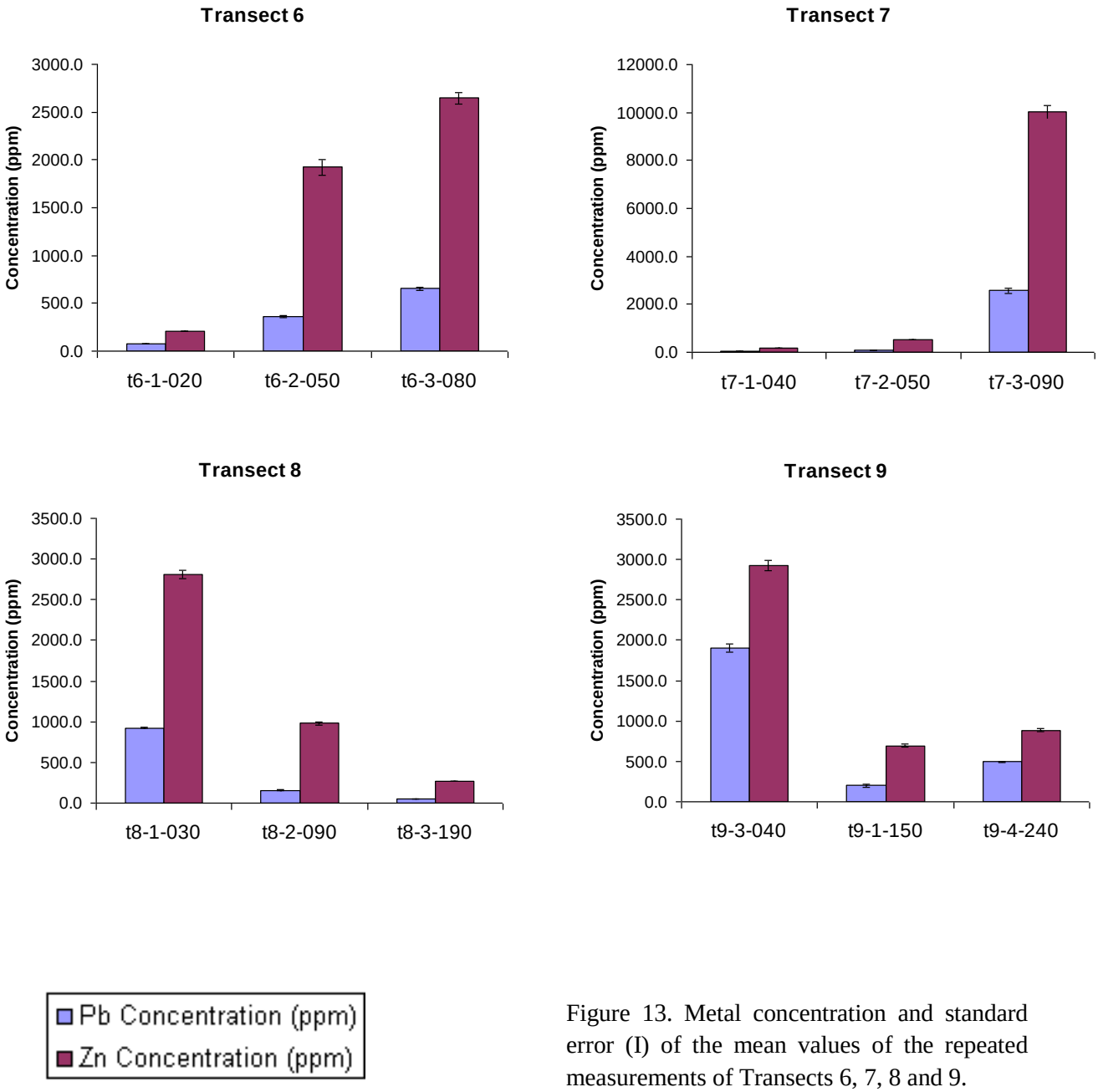

Figure 13. Metal concentration and standard error (I) of the mean values of the repeated measurements of Transects 6, 7, 8 and 9.

- Discussion

The coefficients of variance calculated for the repeated measurements of lead and zinc are low which means that there is not a large variance relative to the mean values within the replicates. These results are considered to be representative for the whole data set as the replicates cover the majority of transects and the samples chosen from each coring are spread along the whole depth of the coring. For this reason the standard error has only been calculated for the replicates. As it can be seen in the graphs (figures 12 and 13) the standard errors of the replicates are insignificant which indicates a high accuracy of the data.

To calculate the standard error of any other measured sample, the same procedure has to be conducted. The standard deviation can be calculated knowing the CV is 8.2 % and 6.5 % for lead and zinc respectively. X represents the mean heavy metal concentration (in the case it is a sample measured just once, it would be the obtained single concentration value for that measurement) according to the following formula:

$SD = CV * X$

4.2.2 Analysis of geomorphologic units

Three major geomorphologic units were differentiated within the Geul catchment: abandoned channel, point bar and floodplain.

According to the study carried out by Heemskerk and Rijnsoever (2005) laboratory results showed that the highest percentage of sand and coarse sand are located in the point bars as well as the highest concentration of organic matter. In the abandoned channels the fraction of silt is higher relative to the point bars and reaches the highest concentrations in the floodplain. Highest concentrations of clay are located in the floodplains.

After the fieldwork performed in this study the results of every coring were sorted within one of the three geomorphologic units according to their characteristics. The summation of the amount of total heavy metals for every single geomorphologic unit was assessed and divided by the number of samples per geomorphologic unit. Therefore, an average value of the metal concentration of each geomorphologic unit was calculated.

- Results

The summation of the amount of total heavy metals for every single geomorphologic unit was assessed and plotted in a graph as follows (figure 12):

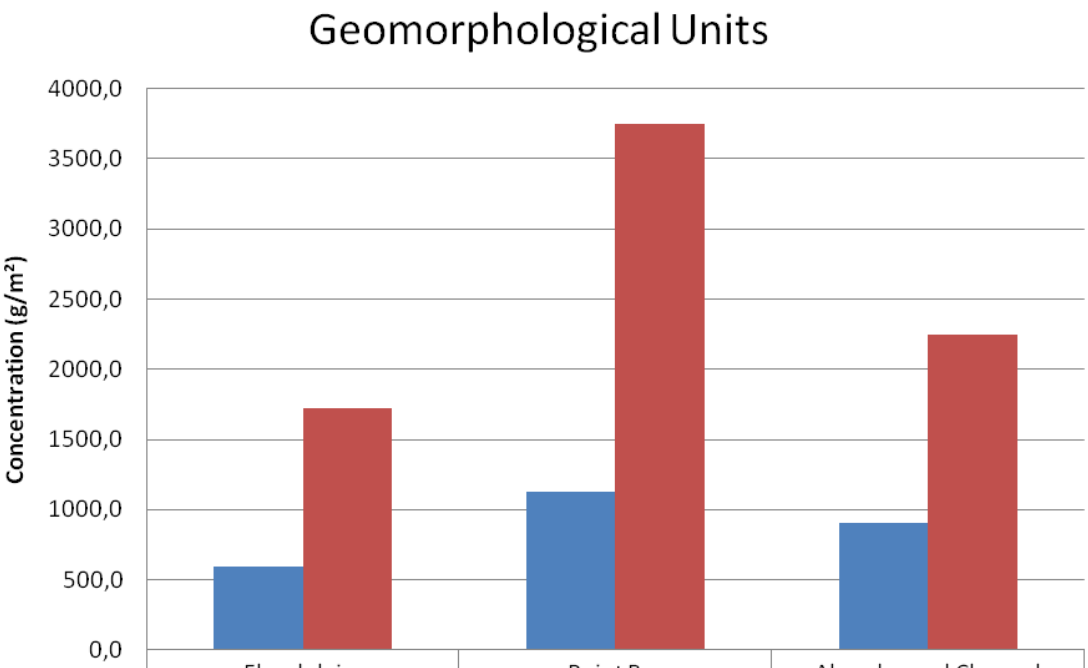

Figure 14. Average zinc and lead content (g/m^2) in every geomorphologic unit (floodplain, point bar and abandoned channel).

Note that in the previous graph (figure 14) the highest content of heavy metals is accumulated in the point bars. The second highest heavy metal concentrations are found in abandoned channels while the less contaminated areas are floodplains.

- Discussion

The grain size distribution in the different geomorphologic units previously mentioned might have an influence on the distribution of heavy metals. According to a study by Heemskerk and Rijnsoever (2005) lead in the floodplain is mostly bound to the fraction smaller than 2 µm (clay) while in the point bars lead is generally bounded to manganese oxides. No trend was found in the abandoned channels. In the point bars the variance of zinc is best explained by the 2 µm-64 µm fraction (silt).

Floodplain areas contain the lowest heavy metal concentration due to the low frequency of inundation and dilution processes with older less contaminated sediments. The further from the river channel the lower the heavy metal concentration. The abandoned channels are areas where water does not normally flow anymore (except during occasional high discharges) and therefore dilution processes cannot take place. Highest heavy metal concentrations are found in point bars. Point bars are the places where contaminants are more active due to erosion-deposition processes and where they first get accumulated before being remobilized due to these processes.

4.2.3 Statistical Analysis of distribution of contaminants over the catchment

The statistical method of linear regression analysis was used to describe the types of existent relationships within the data. To assess an overall inventory of the heavy metal concentration along the valley regression analysis was performed in relation with the Belgian border. Moreover, this method was also used to study the content of heavy metal per coring within each transect with distance to the river.

This technique takes into account that the relationship between 2 variables is linear. As this was not always the case within the data used, the dependent variable Y amount of heavy metal in g/m^2 was Log-transformed so that the relationship between the 2 variables is linear. In order to analyze with further detail results of regression analysis determination coefficients R^2 and the critical F will be discussed.

As it was mentioned before samples were taken down to 2.50 meters deep. However, the statistical analysis of the data was performed with the samples that were collected down to 1.70 meters deep. This was set as the standard depth for the statistical analysis as most of the corings reached this profundity. From this point onwards it was considered to be gravel. Otherwise, as in the statistical analysis summations of the amount of heavy metal are used, amount of heavy metal of different corings could not be compared as they would be quantitatively different.

- Preparation of the data for the statistical analysis

As it is explained in section 3.2 the measuring of the heavy metal concentration of the samples was performed with a hand-held X-Ray fluorescence spectrometer. The obtained concentration values of zinc and lead are expressed in ppm.

The natural background levels of lead and zinc were assessed by visual examination of the data once the whole sampling was completed. Transect 1 (Meerssen) is the furthest located from the mining source. Therefore, according to the results obtained by the XRF measurements, the samples from this location reasonably contain the lowest heavy metal concentrations. Average minimum values from transect 1 were set as standard background values of lead and zinc in soil for the Geul catchment. These are 10 ppm and 40 ppm for lead and zinc respectively.

To calculate the excess concentration values that every sample contained the background values were subtracted from the initial lead and zinc concentration values obtained with the hand-held XRF.

The excess concentration values were multiplied by the bulk density (1.33 g/cm³) to transform the concentrations in ppm to g/m² in order to calculate the whole inventory of heavy metals in the Geul catchment The resultant values in g/m^3 were multiplied by an average value of 0.10 m which is the representative depth per sample taken in the field. All sample values per coring (g/m^2) were then summed up to obtain the total amount of lead and zinc per coring and used in the statistical analysis in section 4.

As an example of these calculation the following graph (figure 15), and table (table 1) show the computation of the data of coring 5 of transect 5 (North Gulpen).

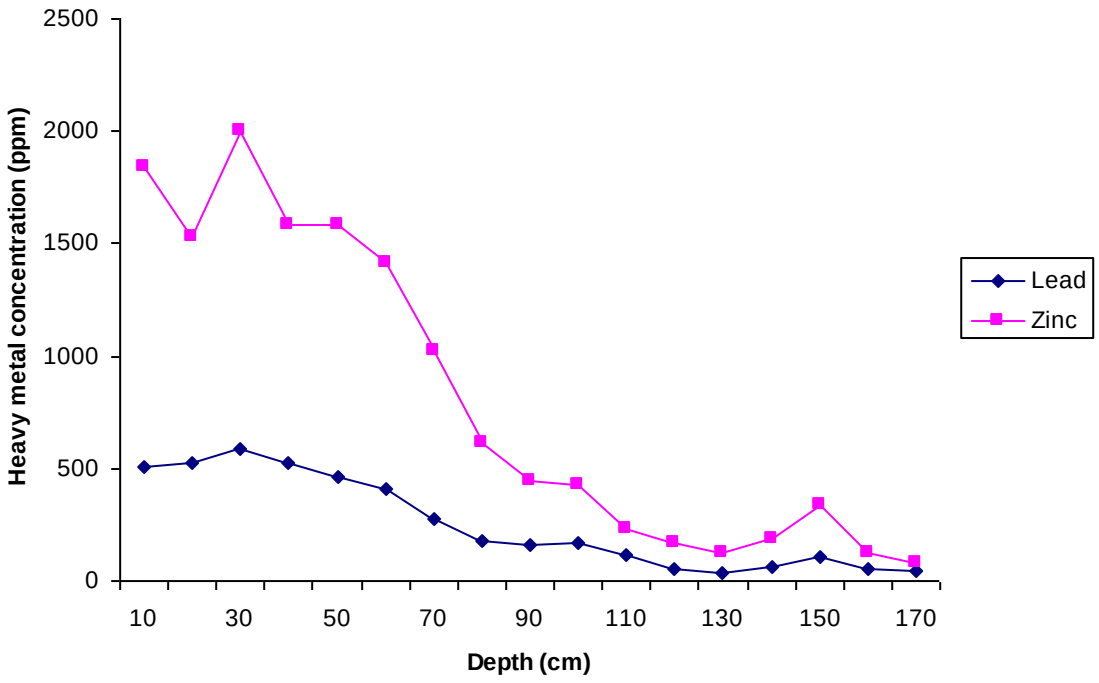

Figure 15. Lead and zinc concentrations (ppm) after subtracting background values. Coring 5, transect 5 (North Gulpen).

Based on these lead and zinc concentrations (ppm) the amounts of lead of zinc in g/m² were calculated as previously explained. The results of transect 5 are shown in table 1. The same calculations were carried out for the rest of the transects.

Table 1. Lead and Zinc concentrations expressed in ppm, g/m^3 and g/m^2 of transect 5 (North Gulpen)

	Lead	Zinc
Total Concentration (ppm) of Coring 5	4276.8 ppm	13698.6 ppm
Total Concentration (ppm)* Bulk density (1.33 g/cm^3)	5688.1 g/m^3	18219.2 g/m^3
Total Concentration (g/m^3) * Depth interval (0,10 m)	568.8 g/m^2	1821.9 g/m^2

- Statistical analysis of contaminants with respect to distance to the source of contamination

In order to analyze the spatial distribution and extent of metal contamination in sediments along the Geul catchment with respect to the source of contamination the total amount of lead and zinc in g/m was calculated. The amount of metals per m^2 per coring (in g/m^2) was multiplied by the representative width of each coring along a transect line. These values were afterwards transformed into its natural logarithm as explained before and used for the regression analysis. The amount of heavy metal represents the dependent variable Y while the independent variable X is the distance from each transect to the source of contamination (considered to be The Belgian border).

- Results

Lead content decreases exponentially (as the metal concentration is log-transformed) with increasing distance to the source of contamination (the Belgian border) presented in figure 16. Zinc behaves in the same way as lead, higher concentrations are found close to the Belgian border and decrease exponentially downstream.

Table 2 shows that similar correlation and determination coefficients as well as critical F value are obtained for lead and zinc when the independent variable of the linear regression analysis is distance to the Belgian border.

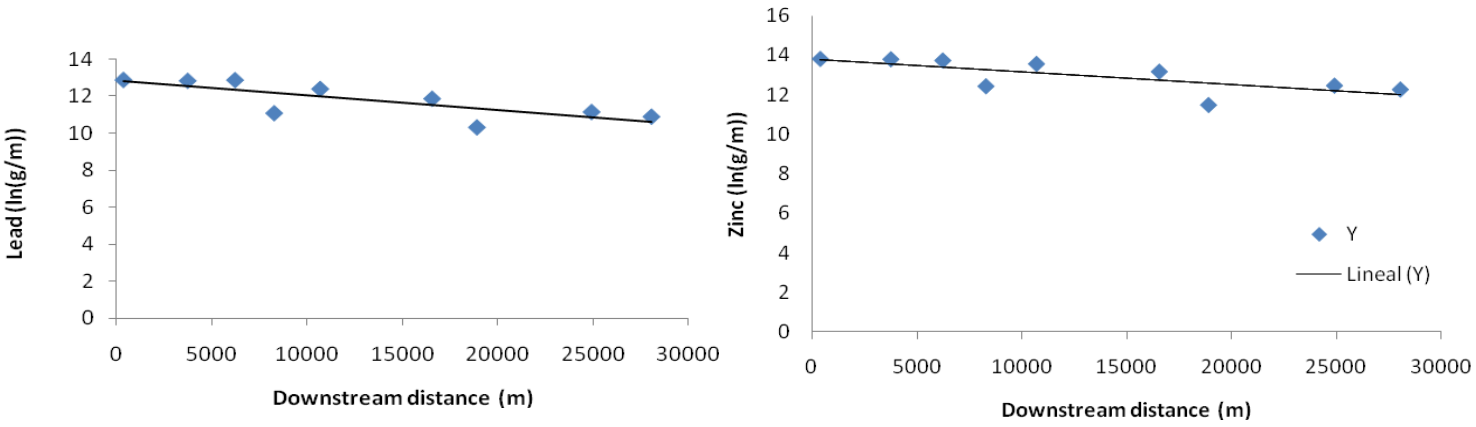

Figure 16. Linear regression analysis graphs of lead and zinc (ln (g/m)) with downstream distance to the source of contamination (Belgian border).

Table 2. Regression analysis results with respect to distance to the border.

Regression Statistics	Zinc	Lead
Determination coefficient R2	0.53	0.60
P value	0.025	0.014
Standard Error	0.61	0.65
Slope	-6.4E-05	-7.85E-05
Intercept	13.82	12.83

- Statistical analysis of contaminants with respect to distance to the river

Regression analysis is used to study the spatial distribution of sediments polluted with zinc and lead along the cross sections performed along the river. The natural logarithms of the heavy metal contents (g/m^2) of the corings per transect represent the dependent variable Y and the independent variable X is represented by the distance from each coring to the river.

- Results

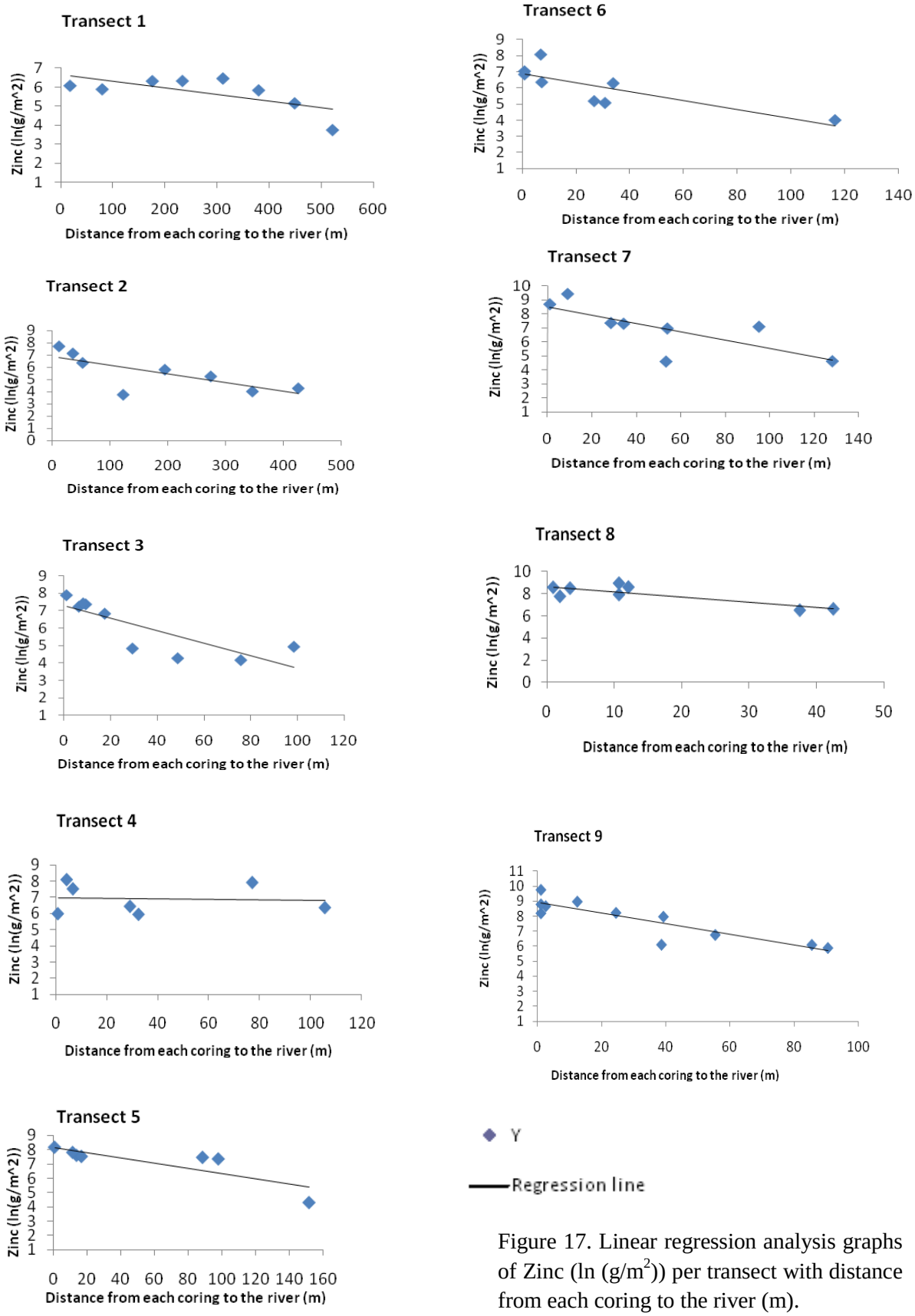

Figure 17. Linear regression analysis graphs of Zinc (ln (g/m^2)) per transect with distance from each coring to the river (m).

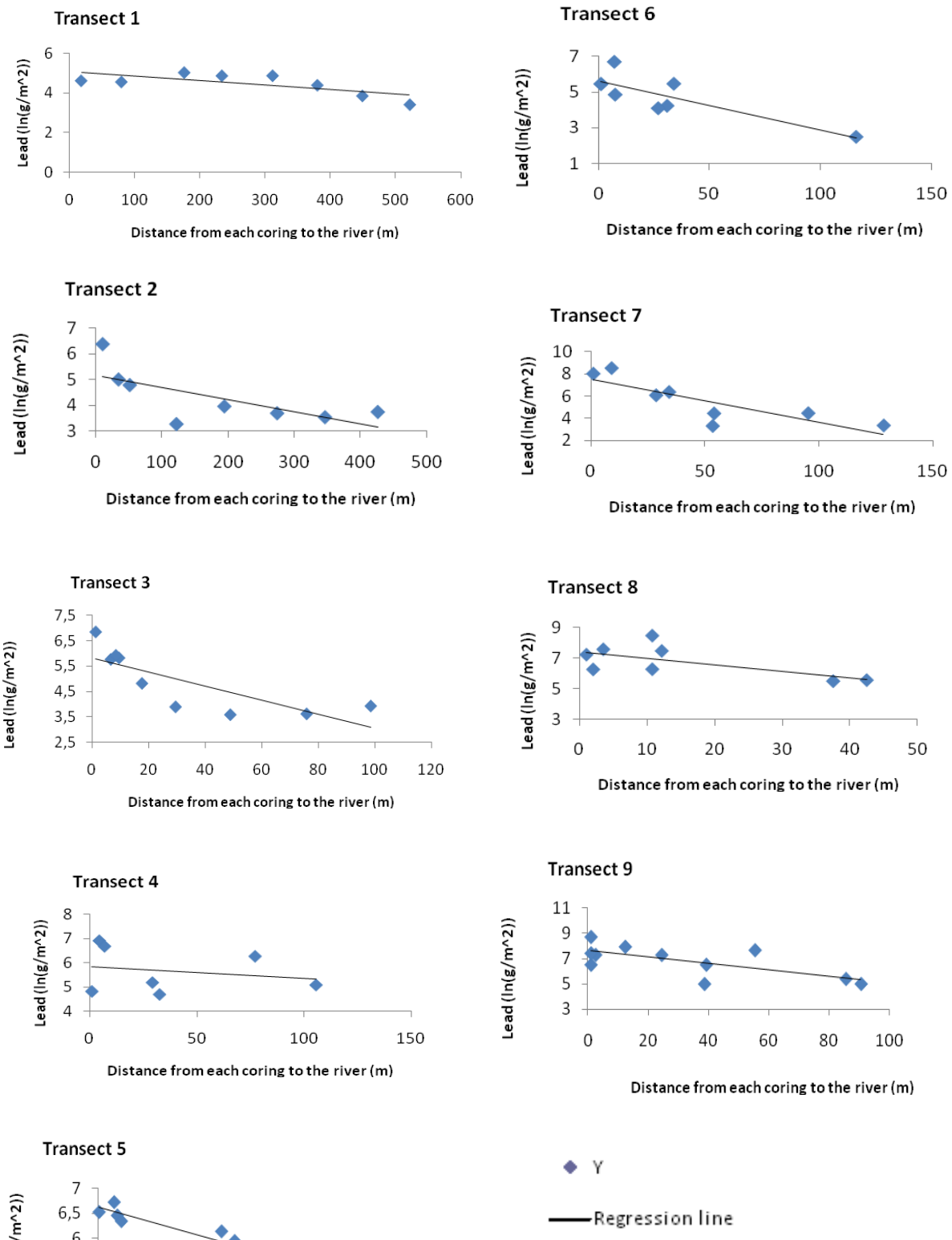

Figure 18. Linear regression analysis graphs of Lead ($ln(g/m^2)$) per transect with distance from each coring to the river (m).

Table 3. Regression analysis results of zinc with respect to distance to the river.

Regression Statistics	Zinc								
Transect number	1	2	3	4	5	6	7	8	9
Determination coefficient R2	0.46	0.55	0.67	0.003	0.68	0.65	0.60	0.71	0.78
P value	0.0643	0.0335	0.0064	0.9	0.0221	0.0159	0.0327	0.0088	0.0003
Standard Error	0.71	1.05	0.91	1.01	0.79	0.84	1.23	0.53	0.66
b	-0.004	-0.007	-0.036	-0.002	-0.018	-0.028	-0.030	-0.049	-0.035
a	6.66	6,83	7,28	6,97	8,16	6.87	8.49	8.65	8.90

Table 4. Regression analysis results of lead with respect to distance to the river.

Regression Statistics	Lead								
Transect number	1	2	3	4	5	6	7	8	9
Determination coefficient R2	0.56	0.49	0.63	0.05	0.89	0.68	0.68	0.43	0.48
P value	0.0330	0.0529	0.0102	0.6419	0.002	0.0112	0.0112	0.0764	0.0183
Standard Error	0.40	0.80	0.78	0.99	0.17	0.76	1.22	0.86	0.53
b	-0.023	-0.047	-0.028	-0.005	-0.008	-0.027	-0.039	-0.043	-0.023
a	5.07	5.16	8.82	5.84	6.63	5.59	7.52	7,43	7.62

Determination coefficients for lead and zinc are within the range of 0.43 and 0.89 except for transect 4 which shows very low values.

- Discussion

The results of the regression analysis considering distance to the source as the independent variable show a clear decrease in heavy metal amount downstream the source of contamination. The source of contamination is located in the upstream part of the Geul River which implies that dilution processes and mixing of the contaminated sediments with non-polluted sediments take place in the downstream direction.

The graphs (figure 16) show that still nowadays higher values of contamination remain upstream. These contaminated sediments are transported downstream when water discharge exceeds the capacity of the river channel producing erosion and deposition of polluted suspended sediment.

These results were expected since, as it was previously mentioned in section 2.2 that other studies (Dennis et al., 2008, Leenaers and Rang, 1989) found the same behavior of decrease of metal concentration in the downstream direction.

The totality of the transects contain higher amounts of zinc than lead. The density of the pollutants may have some influence since ZnS has a lower density than PbS and therefore ZnS will be transported faster and further downstream than PbS. (Heemskerk and Van Rijnsoever, 2005).

As it can be seen in figures 17 and 18, transect 4 and 7 have lower heavy mental content than predicted values. In case of transect 4 it can be explained by its location since some of the corings of this transect were performed in a campsite. Therefore, the soil at this location might have been turned over causing mixing up the layers and decrease in heavy metal concentration. Some corings of transect 7 were located in an alluvial fan. Sediments at this location were therefore affected by the erosion and deposition processes of the hillslope, consequently producing the heavy metal content decrease.

Determination coefficients show that 53% and 60% of the results for zinc and lead regression analyses respectively, are explained by the model. Results are considered to be significant (critical F value is lower than 0.05) and therefore, distance from the pollution source is a useful variable to explain the distribution of the heavy metals along the Geul catchment.

Concerning the regression analysis carried out considering the distance of each coring to the river the results show a general decrease in zinc and lead content when the distance from the river increases.

Table 4 shows the results of the regression analysis in case of lead. Transects 5, 6 and 7 correspond with the highest values determination coefficient and they have a critical value of less than 0.05. Results are significant for transects 1, 3, 5, 6, 7, 9.

The results of the regression analysis for zinc show the highest determination coefficient values in transect 3, 5, 8 and 9 (table 3). The regression is significant for transects 2, 3, 5, 6, 7, 8, 9 (F = 0.05).

The results of the regression analysis of the data collected from transects 3, 5, 6, 7 and 9 are significant for both lead and zinc although no explanation for this pattern has been found (F = 0.05).

5. The CAESAR Model

5.1 Description of the model

CAESAR (Cellular Automaton Evolutionary Slope And River Model) is a two dimensional flow and sediment transport model which can simulate morphological changes in river catchments or reaches. It was initially created by Tom Coulthard (Professor of Physical Geography at the University of Hull) as a part of a PhD project (Coulthard, 2011).

Since then, the model has been further developed. It has been used to model over 100 reaches and catchments over the world on catchment scales within the range of 1 km^2 to 1000 km^2 and reaches up to 40 km in length. It has been utilized in different timescales from individual floods to 10 000 years. (Coulthard, 2011).

The CAESAR model is a catchment cellular model or cellular automata (CA) which represents processes on a two dimensional framework or mesh of grid cells. The following figure (figure 19) shows a general scheme of how CA models work.

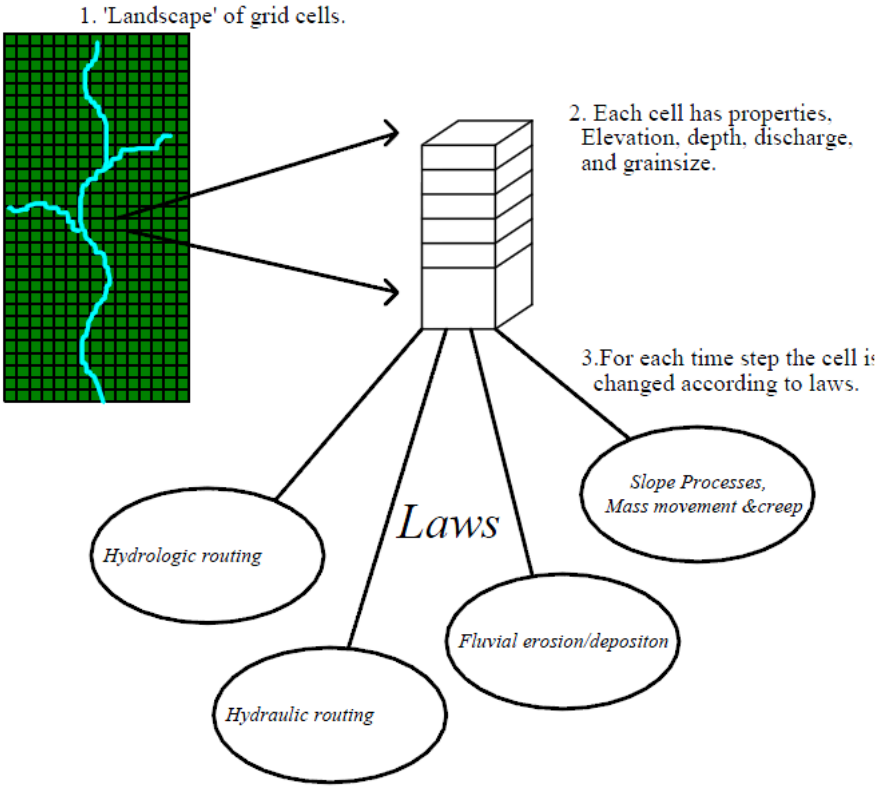

Figure 19. Schematic diagram of the key processes operating in the CA model (Coulthard, 1999).

The model the catchment is represented by a uniform square grid of cells where each of them has its own properties such as elevation, water depth, discharge, vegetation cover and grain sizes fractions. Each time step values of each cell are updated with respect to the neighbouring cells

based on the laws applied in the model. For example, water depth and slope in a certain cell influence the erosion created between that cell and its neighbours. (Coulthard, 1999).

The CAESAR model can be applied in two different modes: catchment mode where an hourly rain data set is needed as an input, or reach mode where discharge can be introduced in the model in one or more points; the latter mode was used in this study.

In the reach mode a DEM file and bedrock file (indicating the depth where the bedrock is situated) are required, both as text files. Discharge and sediment data appear in the same text file in m^3/s and m^3 per time step respectively and can be introduced in different locations of the DEM as mentioned before (Coulthard and Van de Wiel, 2011).

CAESAR uses a "flow-sweeping" algorithm. Water discharge is routed to and distributed according to the water elevation of the donor cell and the bed elevation of the receiving cell. In case of an obstruction the discharge remains in the donor cell to be distributed in different directions in the next sweep. (Van De Wiel et al., 2007).

Flow depth and flow velocity are calculated with Manning's equation:

$$Q[m^3s^{-1}] = UA = \frac{1}{n} h^{2/3} \sqrt{SA}$$

where Q,U, and h are respectively discharge, flow velocity and flow depth, A is the cross-sectional area of the flow ($A = h\ c_w$), S is the average downstream slope, n is Manning's coefficient and c_w is cell width. (Van De Wiel et al., 2007)

Bed load movement and suspended sediment cause erosion and deposition.

Wilcock and Crowe equation is used to model fluvial erosion and deposition for all cells with a flow depth. (Coulthard and Van De Wiel, 2011). Therefore, sediment transport is driven by this equation which calculates transport rates qi, for each sediment fraction i (Van De Wiel et al., 2007).

$$q_i\,[m^3s^{-1}] = \frac{F_i U_*^3 W_i^*}{(s-1)g}$$

where Fi denotes the fractional volume of the i-th sediment in the active layer, U is the shear velocity, s is the ration of sediment to water density, g denotes gravity and W_i is a complex function that relates the fractional transport rate to the total transport rate (Coulthard et al, 2007).

Bed load is transported by cells with lower bed elevations than the previous doner cells as figure 20 a shows. Suspended load transport depends on the differences of water elevation between cells. Suspended load is then routed to the cells where water elevation is lower than the previous cells (figure 20 b). (Van De Wiel et al., 2007).

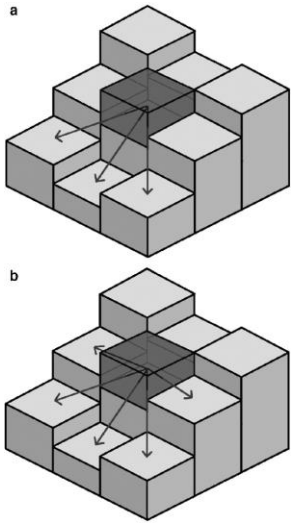

Figure 20: Routing directions for bed load (a) and suspended sediment load (b) (Van De Wiel et al., 2007).

Lateral erosion is calculated by an algorithm that takes into account the local channel curvature with which it calculates the lateral erosion and it distributes the eroded sediments across the channel. (Van De Wiel et al., 2007)

The results given by the model are given in format of a text file as for example water and sediments outputs. Output text files as water depth, grain sizes among others can be imported to ARC-GIS by previously being converted to raster format. (Coulthard and Van de Wiel, 2011).

5.2 Other applications of Caesar

To illustrate its model capacity some of the study cases where the CAESAR model has been applied are mentioned in this section.

The CAESAR model has been used to study the River Swale, Northern England. This is an area with a long history of metal mining. Catchment mode of Caesar model was employed for this study. The DEM used was 50 meters resolution (Coulthard and Macklin, 2003). With the use of TRACER the model results show after a 10 years simulation how the contaminated sediment of the river is spread and deposited downstream (Coulthard et Van de Wiel, 2011).

The Reach mode of the CAESAR model was applied to model a section of the River Teifi. The Teifi is a meandering river situated near Lampeter, Wales (UK). A 10 meter resolution DEM was used. An artificial bed channel was incorporated to the model by lowering the DEM 2 meters. Three simulations were performed in this study focusing on different aspects (Van De Wiel et al., 2007):

1. Flow routing abilities for in-channel and overbank flow conditions (without considering sediment movement).

2. Overbank deposition.

3. Bank erosion and channel migration.

The Waitaki River, a gravel-bed braided river in New Zealand was also a case study for the application of CAESAR. Problems with exotic vegetation invading the braid plain have been occurring during the last 100 years. A vegetation control programme has been put into practice to decrease the inundation hazard, as a result of the high peak lows created by the increase in vegetation. CAESAR was used on its reach mode to simulate morphological changes of the Waitaki. A 50 meter grid DEM was utilized. Vegetation changes were simulated in two ways: allowing vegetation to grow dynamically wherever there was no inundation; and altering lateral erosion rates to simulate the binding properties of riparian vegetation on river banks. (Coulthard et al, 2007).

The CAESAR model was suitable for the case studies previously described as it is able to perform simulations in long term scale, covering a whole catchment and including the relevant parameters that operate in the spatial scale chosen for a certain study. (Coulthard and Van de Wiel, 2011).

6. Simulation of the Geul River with CAESAR model

The modeling carried out in the present study is based on the discharge data registered for the year 2008. Discharge data of the year 2008 (Roer en Overmaas Water Authority) was chosen as an input for the CAESAR model since it was the most recent and complete for all the stations were the input data was collected.

The discharge input data used for the 7 years period simulation was the discharge data of the year 2008, 7 times repeated. Seven locations were selected as the stations supplying the model with input data (see section 6.2.2). The exact coordinates of the seven locations can be found in Appendix 2.

Neither total sediment nor suspended sediment data was introduced in the model due to the lack of data corresponding with the discharge data of the stations. However, the model gives total and suspended sediment results. Suspended sediment results will be further validated in section 6.4.

With the purpose of predicting the amount of zinc and lead after a one year simulation, a seven years simulation was carried out in order to avoid a "spin up" process that the CAESAR model experiences in the first years of the simulation. During the "spin up" process the model starts assuming uniform bed material over the whole catchment. Therefore, it first erodes the finer material leaving the coarser material behind. This happens during the first years of the simulation. Consequently, the resultant sediment at the outlet for the first years is very high but after some years it stabilizes.

Despite the simulation was done for a period of 7 years, when analyzing the sediment budget obtained by the model it was only taken into account the results obtained for the last year of the 7 years simulation as it is the purpose of this study to assess the amount of zinc and lead for the period of 1 year.

In spite the fact that the spin up process does not affect the discharge generated by the model, in order to analyze both sediment and discharge results from the same period of time within the 7 years simulation the analyzed results of discharge in this study belong as well to the last year of the 7 years simulation modeling.

6.1 Model Parameters

The version of the CAESAR model software used for carrying out this study was 6.2g. The input parameters used for this version can be classified in different types based on the way their values were set. A summary of the most important parameters is listed in table 5.

Some of the parameters are standard model parameters as for example parameters involving vegetation, while some others were set after several runs of the model and comparison of results for each of them. Finally, the rest of the parameters were set after calculations with real data and/or by comparison to parameter values found in literature.

Table 5. List of the main parameters in the CAESAR model.

Parameter	Value
Lateral erosion (m/year)	0,5
Min Q for depth Calc (m)	0,25
Water depth threshold above which erosion will happen (m)	0,005
Initial discharge (m3/s)	1
Max erode limit (m)	0,1
Memory limit	3
Init# of scans	50
Max velocity used to calculate Tau (Pa)	5
Vegetation (critical shear stress) (Pa)	100
Vegetation (grass maturity)	1

Lateral erosion rate was set to 0.5 m/year after running the model with several values within the range of 0.3-2 m/year according to lateral erosion values found in a study carried out by De Moor (2006). Among the two methods to calculate lateral erosion method 1 was chosen where lateral erosion includes vertical erosion as the follows expression shows:

Lateral erosion = (vertical erosion * lat rate) / Grain size

The *initial discharge* was set as 1 m^3/s (Wiggers et al. 2006).

Four *grain sizes* were differentiated according to the Diameter limits (mm) USDA Classification and based on the data obtained by Heemskerk and Rijnsoever (2005) included in the appendix 8

(drilling sites) of their study. The proportion of each grain size (as a fraction of 1) was set as the following table shows:

Table 6. Grain sizes and proportions of each of them.

		Grain size (µm)	Proportion
Size 1	Suspended Sediment (clay + silt)	50	0.64
Size 2	Fine sand	150	0.18
Size 3	Sand	300	0.07
Size 4	Coarse sand	1200	0.11

The *settling velocity* for the suspended sediments was set as the default value of 0.0033 m/s.

Min Q for depth Calc is the threshold above which the model will calculate a flow depth. It is dependent upon grid cell size, being 0.1 meter per grid cell size. In this case, the cell size is 25 meters. Therefore, Min Q for depth calculation was set as 0.25. (Coulthard, 2011).

The *max erode limit* (m) determines the maximum amount of material that can be eroded within a cell (Coulthard, 2011). In this study the erode limit is 0.1 m.

The *ini# of scans* refers to the number of scans required to establish the zone around the channel where the model concentrates (Coulthard, 2011). It uses a scanning multiple-flow algorithm that sweeps the area in four directions (north to south, east to west, west to east and south to north) (Coulthard and Macklin, 2003). This parameter was set to 50.

For the model to assess the amount of erosion, the *shear stress (Tau)* is calculated based on flow velocity. In this way, it determines the amount of sediment eroded and moves it according to the discharge in different directions (Coulthard, 2011). This was set as a default value of 5 pascals.

Vegetation is also included in the model by the *critical shear stress* and *grass maturity* (range of 0 to 1) parameters. As it was considered natural vegetation (grass), according to literature the values set for these two parameters were 100 and 1 respectively. (Coulthard, 2011).

6.2 Preparation of the CAESAR model input

6.2.1 Digital Elevation Map

In order for the model to perform the simulations the input data needs to be previously modified to fulfill the model requirements. The starting point was the current elevation map of The Netherlands (AHN) with a resolution of 5 meters.

By using ArcGIS programme the map was transformed and ready to be run in the model. This was achieved according to the following steps. The area of the Geul River catchment was selected from the whole map. After trying with different resolutions (from higher to coarser resolution) the only one accepted by the model (due to the large size of the catchment area) was 25 meters resolution. The catchment of the river Geul was cut out from the AHN map. To select the floodplain from the whole catchment area of the river Geul the scale was modified leaving out values over 125 meters. The main channel line was manually drawn in some parts and lowered by 2 meters. Sinks were removed and some walls were added in the input and output cells to force the water to properly flow in and out of the channel.

A bedrock file was created subtracting 2 meters from the final DEM of the Geul catchment.

The CAESAR model is designed so the main channel flows from left to right (Coulthard, 2011). This requirement implied some more changes to the former DEM. To get a flow direction from left to right, the outlet of the catchment must be on the right side of the DEM. In order to get this the catchment had to be rotated 180° as figure 21 shows.

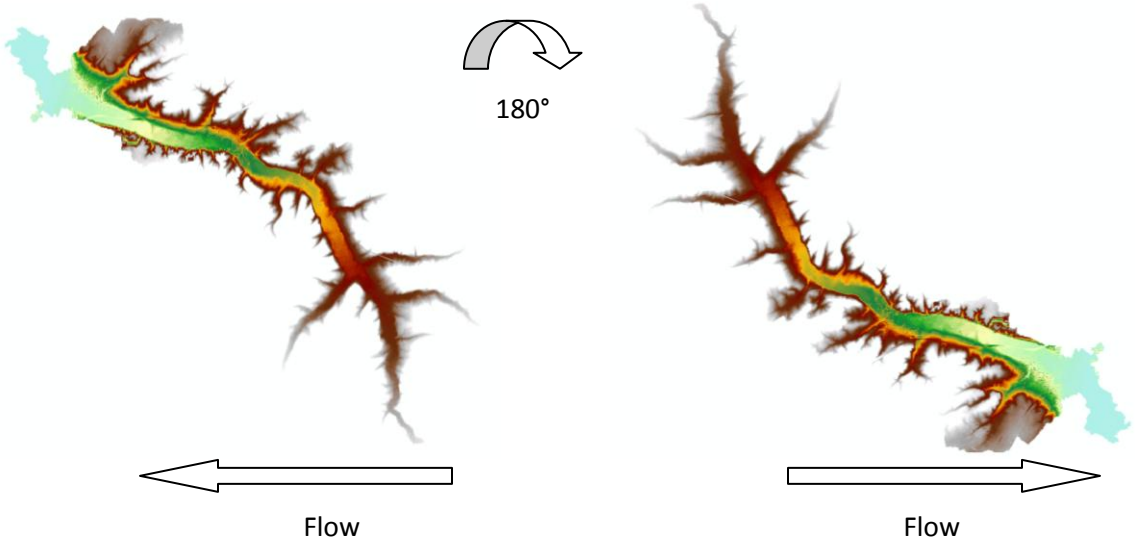

Figure 21. Rotation of the catchment.

To prevent resampling of the DEM the rotations had to be done in multiples of 90° (Coulthard, 2011). Therefore the catchment was rotated 180°.

Once the flow direction was set from left to right, the catchment exit point needed to be on the right hand end of the DEM as it is one of the prerequisites of Caesar Model. In this case the outlet of River Geul points South. Therefore, the DEM was clipped on the right side as it can be seen in figure 22.

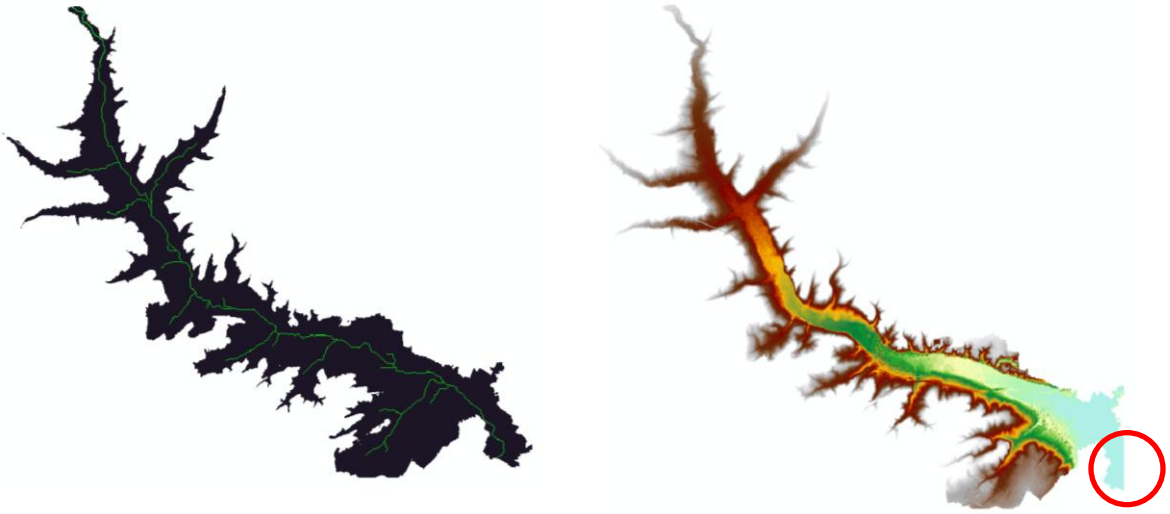

Figure 22. Left image shows the main channel of the Geul River. On the right the DEM of the Geul River shows the clipped part of the catchment within the red circle.

After these modifications the final DEM resulted in a file with total number of 514386 cells. Among this total, the number of active cells is 96306. The surface elevation varies within the range between 37 and 131 meters above the sea level.

6.2.2 Discharge Data

The Reach mode of the CAESAR model requires an input text file with the first column corresponding to time steps, water discharge (m^3/s) in the second column and inputs for the different grain size fractions (in m^3 corresponding to each time step) in the 6^{th} to 14^{th} columns. In this study, the introduced text files contained hourly discharge values in m^3/s corresponding with each time step. No sediment data was introduced due to the unavailability of data for each of the different grain sizes. Therefore, the obtained sediment output values are generated by erosion and deposition processes after the discharge data is entered in the model.

Locations of input discharges in the model correspond with the location of the discharge monitoring stations of the Roer and Overmaas Waterboard where discharges of the Geul River and its tributaries are measured (see Appendix 2).

Due to the lack of discharge data at the lowest half part of the Geul catchment two extra discharge inputs, Downstream 1 and 2, were added along the main channel. The discharge locations introduced into the model are shown in the following map (figure 23):

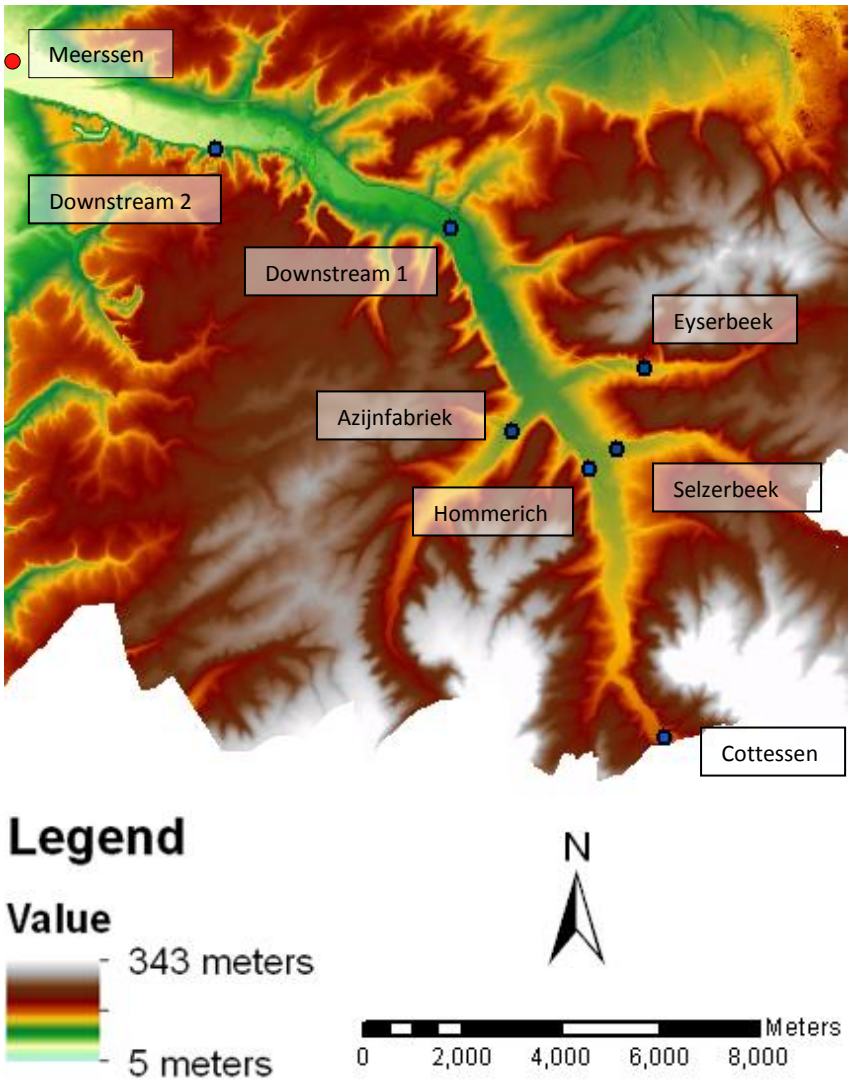

Figure 23. Locations of Caesar input discharges along the Geul catchment (blue dots). Downstream discharge station at Meerssen (red dot).

Due to the fact that both Cottessen and Hommerich are located at the main channel some calculations were needed to get the set of discharge data values corresponding to Hommerich location to avoid adding double discharge values to the model. Assuming an average flow velocity of 1 m/s (Wiggers et al. 2006) and measuring the distance from Cottessen to Hommerich measure stations (8,200 meters) it was possible to calculate the time delay at which discharges at Cottessen reach Hommerich. Therefore, hourly discharge data set of Cottessen was subtracted from hourly Hommerich data set at two hours shift and the resulting data set introduced at Hommerich.

To calculate the last two input discharge locations, Downstream 1 and 2, several calculations were necessary to set the corresponding discharge values to realistic values. The discharges for the two downstream locations 1 and 2 were calculated using available data from a discharge station at Meerssen (located downstream the Geul catchment next to its confluence with the Meuse river). Considering a flow velocity of 1 m/s and a distance of approximately 22 km from the location at which all the upstream discharges merge (Azijnfabriek, Eyserbeek, Hommerich, Selzerbeek and Cottessen) results in 6 hours of travel time from the mentioned location to Meerssen station. Therefore, subtracting upstream discharge values where water merges to Meerssen discharge values at 6 hours shift it is possible to calculate the remaining discharge values corresponding to an input at the downstream part.

However, in order to make it more equally spatial distributed the calculated discharge values were divided by two and two downstream inputs set of values were introduced in the model. Downstream 1 is located 7 km from the upstream inputs merging point. Therefore, it corresponds to a shift of 2 hours in discharge data. Downstream 2 is located 7 km further downstream 1 with an added 2 hours shift in discharge values. In this way and taking into consideration a flow velocity of 1m/s a peak discharge value occurring at downstream 1 appears at downstream 2 location 2 hours later. Consequently, the former peak discharge value will appear at Meerssen discharge station 4 hours later.

6.3 Results

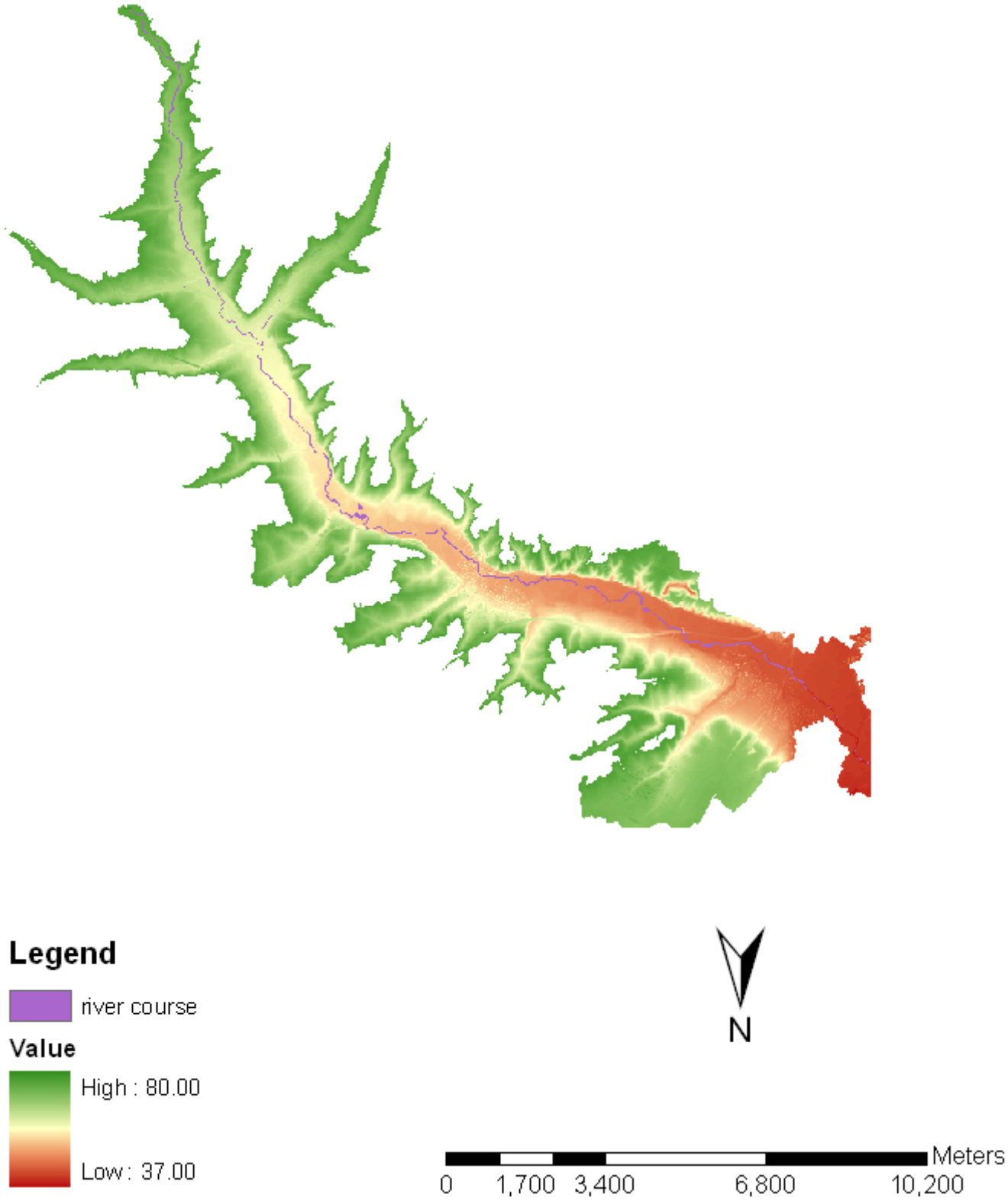

Figure 24. River course (purple) after 1 year simulation with data of 2008 overlapping the DEM (elevation values are shown in meters).

The above figure (figure 24) is the final state of the course of the river after 1 year simulation with discharge input data of 2008. This was overlapped with the former DEM introduced as an

input in CAESAR. It can be noticed that both maps are 180° rotated to be introduced as an input for CAESAR. When analyzing the previous image in further detail it can be seen how some parts of the river experienced meandering processes in comparison to the former river course (DEM). However, as the study of meandering processes of the Geul River is not the aim of this study figure 24 is intended to be an ilustration of the final state of the river after 1 year simulation with CAESAR model.

In the following graph (firgure 25), the discharge at the outlet of the Geul river is showed for the year 2008.

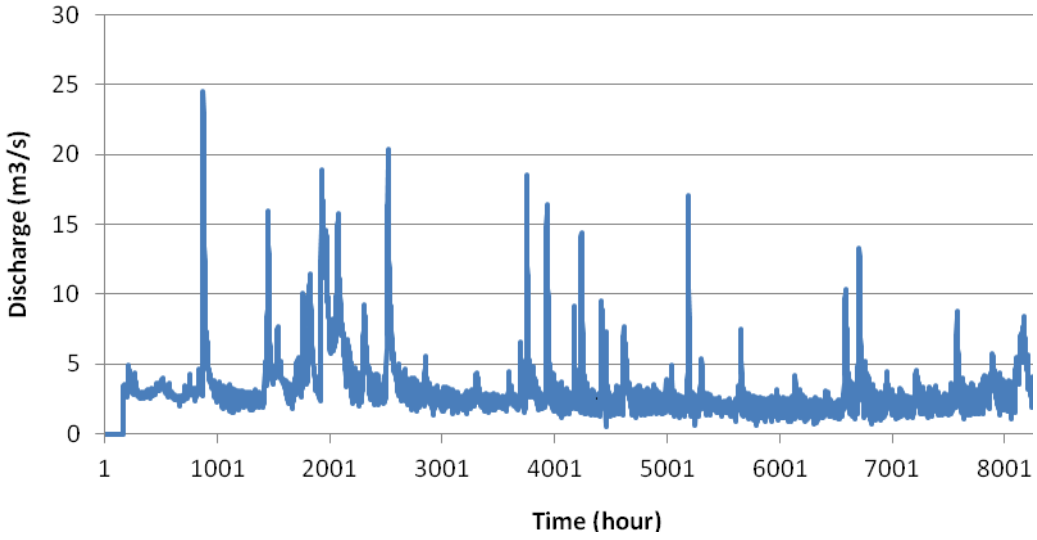

Figure 25. Discharge (m^3/s) at the outlet of the Geul river after a one year simulation.

The graph shows the discharge at the outlet of the river for the input data of 2008. As it can be seen, the discharge stays approximately within the range of 1-4 m^3/s but for several peaks that reach 20-25 m^3/s. These results will be validated with dicharge data from Meerssen station during the same period of time in section 6.4.

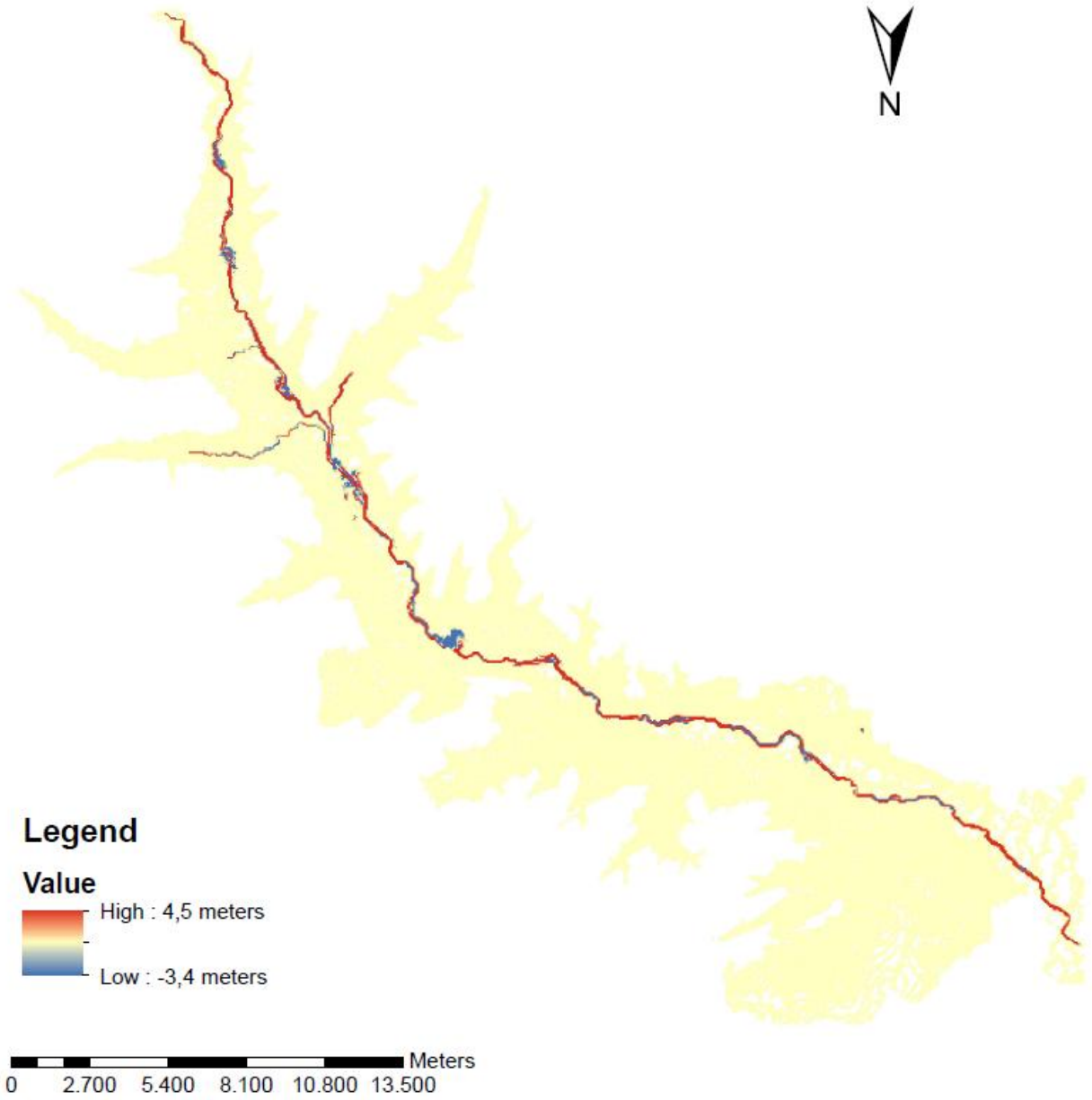

Figure 26. Elevation difference map of the Geul river after one year simulation. Positive values indicate erosion and negative values correspond to deposition.

Figure 26 shows that erosion values are higher than deposition values. These results were expected due to the fact that the model produces a sediment budget in the outlet of the river after the simulation. Erosion is mostly concentrated in the main channel. Areas where deposition takes place will accumulate sediment and will act as future sources of contamination that will again be eroded continuing in a cycle of erosion and deposition.

As explained before, a 7 years run was performed to analyze the sediment obtained at the outlet of the Geul River for the year 2008. The spin up process generates high sediment values during the first years. As proof of this process table 7 shows the suspended sediment values obtained per year after a 7 years simulation.

Table 7. Total and suspended Sediment values per year at the outlet of the Geul River after a 7 years simulation with the CAESAR model.

Simulation time for input data from 2008	Suspended sediment at the outlet (m^3)	Total sediment at the outlet (m^3)
1st year	172,433	434,066
2nd year	219,570	567,924
3rd year	254,110	463,491
4th year	140,788	259,665
5th year	74,529	138,915
6th year	68,517	129,034
7th year	59,173	109,014

In order to avoid overestimation of the sediment obtained by the modeling at the outlet of the River Geul due to the spin up process, the calculations to assess the amount of heavy metals in one year were carried out with the total sediment volume obtained in the last year of the 7 year simulation with the CAESAR model.

The total sediment volume at the outlet obtained by the model in the last year of 7 years simulation is 109,014 m^3.

Considering a bulk density of 1,330 kg/ m^3 the total sediment at the outlet is 144.9 10^6 kg.

According to the soil samples collected and analyzed in this study the average concentrations of lead and zinc in the Geul catchment are 100 ppm and 400 ppm respectively.

Therefore, considering a total sediment value at the outlet of 144.9 10^6 kg and the average concentrations of lead and zinc, the amount of lead and zinc obtained in one year can be assessed:

Total lead at the outlet of the 2008 simulation: 14.5 tons.

Total zinc at the outlet of the 2008 simulation: 57.9 tons.

6.4 Validation

Validation of fluvial models can be complex since these models generate data that cannot be directly measured in the field as for example erosion and deposition data (Coulthard et Van de Wiel, 2011). Discharges at the outlet of the Geul River obtained after one year simulation using the CAESAR model can be compared with measured discharges at Meerssen in 2008 (Figure 27).

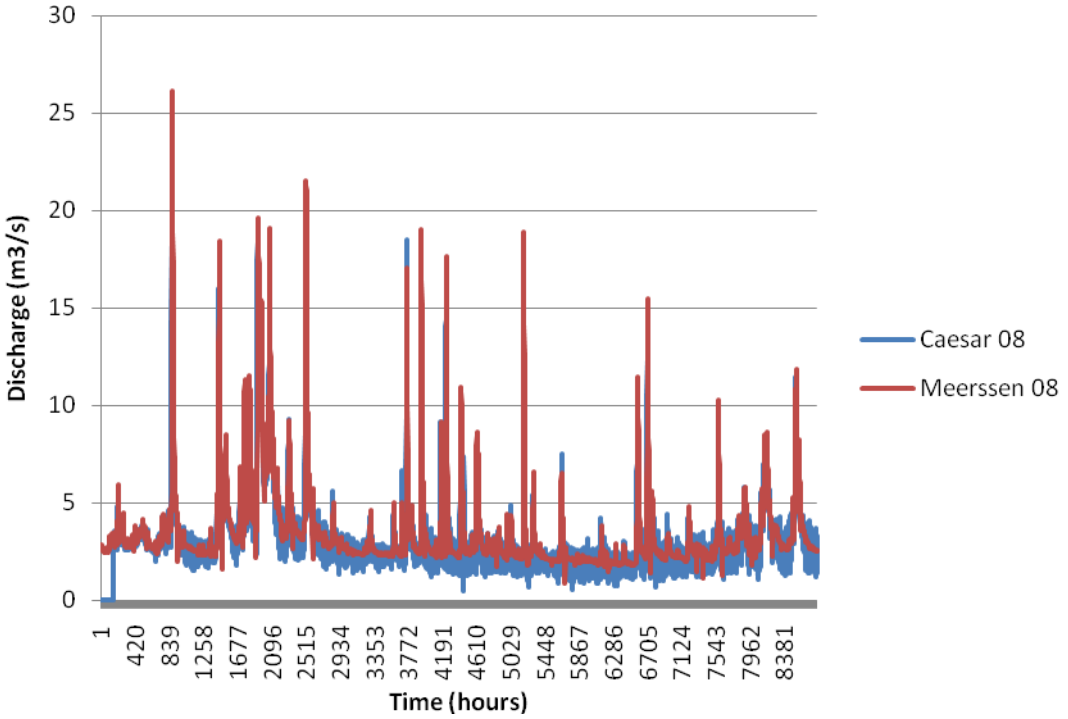

Figure 27. Discharge (m^3/s) obtained at the outlet of Geul River after one year simulation (blue colour) and discharge (m^3/s) measured at Meerssen in 2008 (red colour).

In order to validate the sediment results of the model, values of suspended sediment of the year 2008 at the outlet are compared with values of suspended sediment from 1983 (Leenaers, 1989). According to the values obtained in the study carried out by Leenaers (1989) total suspended sediment output at the confluence with the river Meuse for the year 1983 (Meerssen) is 30,656 tons of suspended sediments. This value corresponds to the totality of the catchment (380 km^2). The present study has focused on the Dutch part of the catchment. Therefore, in order to compare the result obtained by Leenaers (1989) with the results of the current study and considering that the Geul catchment occupies 240 km^2 in The Netherlands, it can be said that the corresponding suspended sediment for the Dutch part is 19,362 tons.

The resultant output of suspended sediment from the last year of a 7 year simulation with the CAESAR model gives a value of 59,173 m^3 at the outlet of the Geul River. Considering that the bulk density of suspended sediment is 1,600 kg/m^3 (Morrow and McConchie, 2010) the output suspended sediment from the model simulation results in 94,677 tons.

6.5 Discussion

Figure 27 shows that discharge results of the modeling are very similar to the measured ones at Meerssen in 2008. Peaks occur at the same time and approximately within the same range of discharge. Both discharge results from the CAESAR model (figure 25) and measured discharge at Meerssen vary within the range of 1-4 m^3/s except for several peaks that reach 20-25 m^3/s. As it can be seen in figure 27 the CAESAR model predicts lower values of discharge than the measured ones in Meerssen. These can be attributable a lower baseflow as calculated by the model.

The elevation difference resulting after erosion and deposition processes in the modeling of the year 2008 varies within the range of approximately -3 to 4 meters. As it refers to elevation difference, negative and positive values correspond with deposition and erosion respectively. As it can be seen in figure 26 erosion processes take place in the main channel, outer bends of the river as well as in the inner part of the main channel, while deposition happens in the lower parts of the catchment and inner bends of the river. It can be observed that in the upper part of the river erosion is slightly higher than in the rest of the river. The reason for this can be that the upstream part of the river has a higher slope than the downstream part.

According to a study carried out by De Moor (2006) for the year 2000 the sediment obtained at the outlet 30,674 tons for the whole catchment (380 Km^2).

The results of the present model give a total sediment value at the outlet of the catchment (considering only the Dutch part of the catchment) of 144.9 10^3 tons which is around 5 times larger than the results obtained by De Moor (2006). Due to the fact that in this study only the Dutch part of the catchment is considered (240 Km^2), the results of the modeling were expected to be around 30% smaller than the mentioned ones by De Moor (2006).

The reason for this could be that the CAESAR model uses a DEM with 25 meter resolution, which means that the river that is being modeled is twice as wide at least than in reality, which is approximately from 8 to 15 meters. In some occasions, it can even be more than twice wider as in some of the bends the river uses two pixels in a row that increase the width, and consequently the sediment produced in that area. Other irregularities in the DEM can also contribute to the high result in total sediment.

Furthermore, the 'spinning up' process can still have had some influence in the sediment results of the last year of the 7 years simulation.

The suspended sediment results of the modeling for the last year of the 7 years simulation for the year 2008 (94,677 tons) are approximately 3 times larger than the ones obtained in the study carried out by Leenaers (1989) for the year 1983 (30,656 tons). As it happens with the results for the total sediment, the suspended sediment created by the model could also be affected by the spinning up process and irregularities of the DEM producing an overestimation of the results.

As it has been previously explained there is an overestimation in the modeling results. For this reason, due to the fact that the assessed amounts of lead and zinc (14.5 and 57.9 tons respectively) for the year 2008 were calculated based on the total sediment results of the CAESAR model, it is expected that these results are also overestimated by 3-5 times.

7. Conclusions

The analysis of the data compiled for this study shows that soil vertical profiles present higher concentrations of zinc than lead, probably due to the earlier start of zinc industrial mining at La Calamine in 1806.

XRF analysis results of the samples collected allowed assessment of the content of zinc and lead per geomorphologic unit resulting in floodplains containing the lowest heavy metal concentrations, followed by abandoned channels. Highest heavy metal concentrations are found in point bars as they are the areas with more dynamic erosion-deposition processes.

The statistical analysis carried out in the present study shows a decrease in heavy metal content in the downstream direction. This can be explained by dilution processes and mixing of the contaminated sediments with non polluted sediments further from the source of contamination (located upstream). Therefore, the significant results obtained in the statistical analysis conclude that distance to the Belgian border is a useful variable to explain the distribution of the heavy metals along the Geul catchment.

Regarding the statistical analysis considering distance of each coring to the river, the results show a general decrease in zinc and lead content when the distance from the river increases. These results are significant for the majority of transects but determination coefficients are lower than the ones obtained in the regression analysis considering the distance to Belgium as the independent variable. Therefore, distance to the river is considered to be a less useful variable than distance to the Belgian border to explain the distribution of the heavy metals along the Geul catchment.

Results from the modeling and validation with measured data in Meerssen show that CAESAR model predicts lower values of discharge than the measured ones. Despite that, values of discharge are within the same range (1-4 m^3/s) in both measured and modeled values and peaks occur approximately at the same time.

Total sediment budget generated by the model is 144.9 10^3 tons which is around 5 times larger than the results obtained by De Moor (2006) for the year 2000. Suspended sediment generated by the model reaches a value of 94,677 tons, 3 times larger than results found in the study carried out by Leenaers (1989) for the year 1983. For both sediment budgets (total and suspended sediment) the CAESAR model gives an overestimated result. The reason for this could be that the model uses a DEM with 25 meter resolution. The real width of the river is approximately 8 to 15 meters, which means that the model is using a river which is at least twice as wide as it is in reality. Consequently, the sediment generated is larger. Other irregularities in the DEM and the 'spinning up' process the model carries out during the first years of the simulation can make an influence in the final sediment results.

The assessed exports of lead and zinc from the Geul floodplain for the year 2008 were 14.5 and 57.9 tons respectively. These calculations were based on the total sediment results of CAESAR model. Therefore, as the generated sediment budget is overestimated by the model, these results are expected to be overestimated as well.

In spite of that, based on these results it can be noted the extent of heavy metal contamination in the Geul River. Large amounts of zinc and lead persist at present in the sediments of the

catchment which leads to think about a very slow natural decontamination of the river. Further research on decontamination of polluted sediments in rivers such as in the Geul catchment and the improvement of models which provide more accurate and reliable results is needed to further understand heavy metal contamination in fluvial systems.

References

Altman, D. G., Bland, J. M. (2005) Statistics Notes: Standard deviations and standard errors. BMJ 331, 903.

Bendel, R. B., Higgins, S. S., Teberg, J. E., Pyke, D. A. (1989). Comparison of skewness coefficient, coefficient of variation, and Gini coefficient as inequality measures within populations. Oecologia 78, 394-400.

Black, K., 2008. Business Statistics: Contemporary Decision Making, 5th Edition. University of Houston, Clear Lake, TX.

Coulthard, T. J. (1999). Modelling Upland Catchment Response to Holocene Environmental Change. Unpublished Phd Thesis, School of Geography, University of Leeds, U.K. 181pp. Published online in: http://www.coulthard.org.uk/downloads/coulthard%20thesis%20chapter4.pdf

Coulthard, T. J. (2011). Using CAESAR to simulate morphological changes in rivers. Published online in: http://www.coulthard.org.uk/caesardownloads.html

Coulthard, T.J., Hicks, M.D., Van De Wiel, M.J., 2007. Cellular modelling of river catchments and reaches: advantages, limitations and prospects. Geomorphology 90, 192–207.

Coutlhard, T. J., Macklin, M., G. (2003). Modeling long term contamination in river systems from metal mining. Geology 31, No. 4, 451-454.

Coulthard, T.J., Van De Wiel, M.J. (2011) The Cellular Automaton Evolutionary Slope And River model (CAESAR). Published online in: www.coulthard.org.uk/downloads/CAESAR_instructions2.pdf

De Moor, J. J. W. (2006). Human impact on Holocene catchment development and fluvial processes - the Geul River catchment, SE Netherlands. Ph.D. thesis, Vrije Universiteit Amsterdam.

De Moor, J.J.W., Verstraeten, G. (2008). Alluvial and colluvial sediment storage in the Geul River catchment (The Netherlands) - Combining field and modelling data to construct a Late Holocene sediment budget. Geomorphology 95, 487–503.

De Moor, J.J.W., Van Balen, R.T., Kasse, C. (2007). Simulating meander evolution of the Geul River (The Netherlands) using a topographic steering model. Earth Surface Processes and Landforms 32, 1077–1093.

Dennis, I. A., Coulthard, T. J., Brewer, P., Macklin, M. G. (2008). The role of floodplains in attenuating contaminated sediment fluxes in formerly mined drainage basins. Earth Surface Procesess and Landforms. Published online in Wiley InterScience (www.interscience.wiley.com). DOI: 10.1002/esp.1762

Hassani, H., Ghodsi, M., Howell, G. (2010). A note on standard deviation and standard error .Teaching Mathematics and Its Applications 29, 108-112.

Van Heemskerk, J., Van Rijnsoever, R. (2005). The influence of migration of the river Geul on the temporal and spatial distribution of heavy metals. M.S. Thesis. Utrecht University, The Netherlands.

Hürkamp, K., Raab, T., Völkel, J. (2009). Two and three-dimensional quantification of lead contamination in alluvial soils of a historic mining area using field portable X-ray fluorescence (FPXRF) analysis. Geomorphology 110, 28-36.

LearnXRF.com (2011): http://www.learnxrf.com/BasicXRFTheory.htm

Leenaers, H. (1989). The dispersal of metal mining wastes in the catchment of the river Geul (Belgium - The Netherlands). *Netherlands Geographical Studies* 102. Koninklijk Aardkundig Genootschap/Geografisch Instituut Rijksuniversiteit Utrecht, Amsterdam/Utrecht, 200 pp.

Leenaers, H., Rang, M. C. (1989). Metal dispersal in the fluvial system of the River Geul: The role of discharge, distance to the source, and floodplain geometry. Sediment and the Environment (Proceedings of the Baltimore Symposium, May 1989). IAHS Publ. nl. 184.

Morrow, F. and McConchie, J. (2010). Hutt River Mouth. Fluvial Sediment Transport. Opus International Consultants Limited. Published online in: http://www.gw.govt.nz/assets/council-publications/Hutt%20River%20Mouth%20-%20Fluvial%20sediment%20transport.pdf

Render, B., Ralph, S.M., Michael, H.E. 2008. Quantitative analysis of management. Pearson Custom Business Resources Series.

Science Education Resource Centre at Carleton College (SERC). Geochemical Instrumentation and Analysis (2011): http://serc.carleton.edu/research_education/geochemsheets/techniques/XRF.html

Stam, M. H. (1999). The Dating of Fluvial Deposits with Havy metals, ^{210} Pb and ^{137}Cs in the Geul Catchment (The Netherlands). Phys. Chem. Earth (B), Vol. 24, No. 1-2, 155-160.

Swennen, R., Van Keer, I., De Vos, W. (1994). Heavy metal contamination in overbank sediment of the Geul river (East Belgium): Its relation to former Pb-Zn mining activities. Environmental Geology 24, 12-21.

Tom Coulthard, Professor of Physical Geography, University of Hull, UK. Fluvial Geomorphology and the CAESAR model (2011): http://www.coulthard.org.uk/CAESAR.html

Van De Wiel, M.J., Coulthard, T.J., Macklin, M.G. and Lewin, J. (2007). Embedding reach-scale fluvial dynamics within the CAESAR cellular automaton landscape evolution model. Geomorphology 90, 283–301.

Wiggers, R., Van den Hoek, T., Van Maanen, B., Higler, B., Van Kleef, H. (2006). Some rare and new Caddis flies recorded for The Netherlands (Trichoptera). Nederlandse Faunistische Mededelingen 25.

Appendices

Appendix 1

Coordinates of drilling locations.

Transect	Coring	X	Y
1	1	182551	320736
1	2	182531	320660
1	3	182503	320603
1	4	182476	320541
1	5	182443	320473
1	6	182418	320418
1	7	182382	320359
1	8	182335	320283
2	1	184749	320170
2	2	184753	320090
2	3	184748	320016
2	4	184745	319937
2	5	184736	319864
2	6	184740	319779
2	7	184842	319780
2	8	184861	319744
3	1	188610	318402
3	2	188602	318371
3	3	188593	318352
3	4	188582	318330
3	5	188570	318310
3	6	188612	318427
3	7	189379	317932
3	8	189395	317923
3	9	189412	317925
4	1	189584	317219
4	2	189657	317225
4	3	189682	317247
4	4	189544	317216
4	5	189528	317172
4	6	189459	317107
4	7	189464	317130
5	1	190856	314510
5	2	190921	314523
5	3	190989	314517
5	4	191015	314525
5	5	191048	314503
5	6	191115	314547
5	7	191197	314581
6	1	192381	312824
6	2	192361	312797

Transect	Coring	X	Y
6	3	192364	312806
6	4	192218	312910
6	5	192258	312766
6	6	192226	312783
6	7	192247	312828
6	8	19218	312697
7	1	192642	311402
7	2	192661	311401
7	3	192690	311384
7	4	192704	311388
7	5	192733	311382
7	6	192764	311370
7	7	192799	311365
7	8	192832	311379
8	1	192842	309557
8	2	192827	309582
8	3	192780	309600
8	4	192874	309540
8	5	192770	309611
8	6	192722	309618
8	7	192703	309621
8	8	192672	309628
9	1	193536	307809
9	2	193489	307807
9	3	193460	307830
9	4	193468	307789
9	5	193448	307749
9	6	193450	307722
9	7	193462	307763
9	8	193443	307715
9	9	193437	307679
9	10	193459	307621
9	11	193459	307619

Appendix 2

Location of input discharges in CAESAR model.

Location	X	Y
Cottessen	193609	307708
Hommerich	192116	313154
Meerssen	178825	322436
Eyserbeek	193211	315195
Selzerbeek	192668	313552
Azijnfabriek	190542	313924

Appendix 3

Vertical Profiles

Transect 1

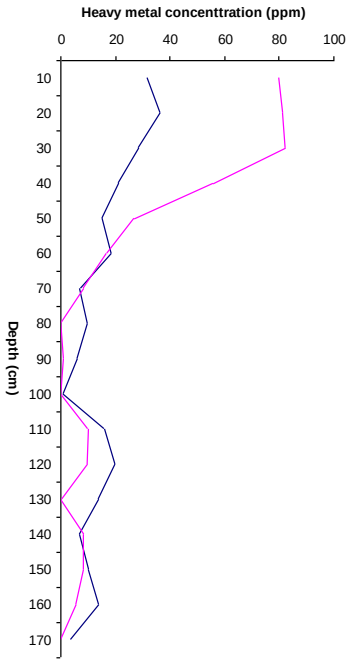

Figure 1. Metal concentration profile

Transect 1 coring 1

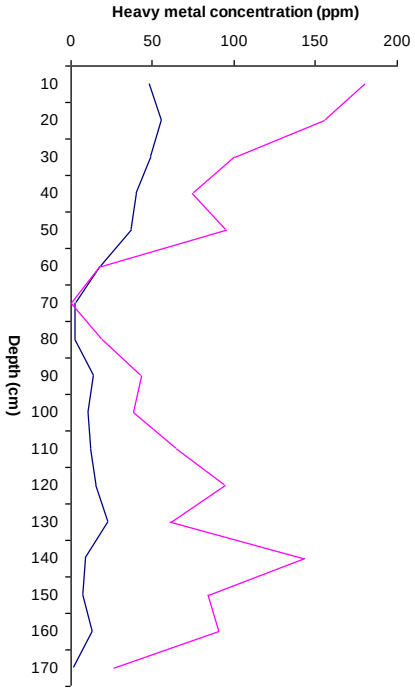

Figure 2. Metal concentration profile

Transect 1 coring 2

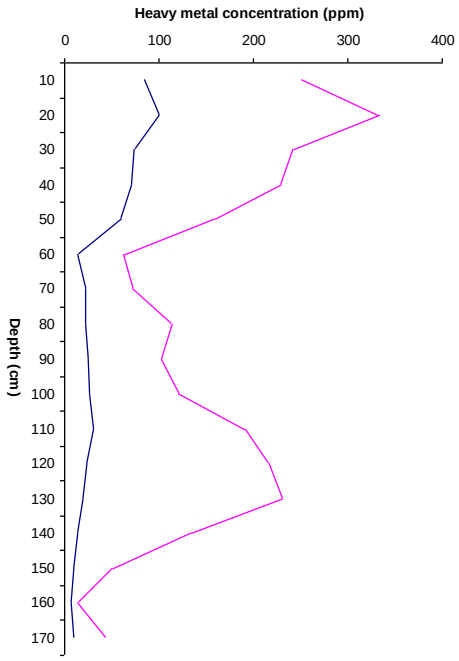

Figure 3. Metal concentration profile

Transect 1 coring 3

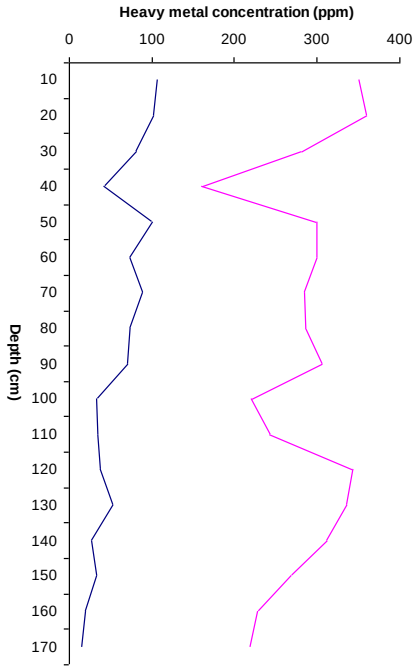

Figure 4. Metal concentration profile

Transect 1 coring 4

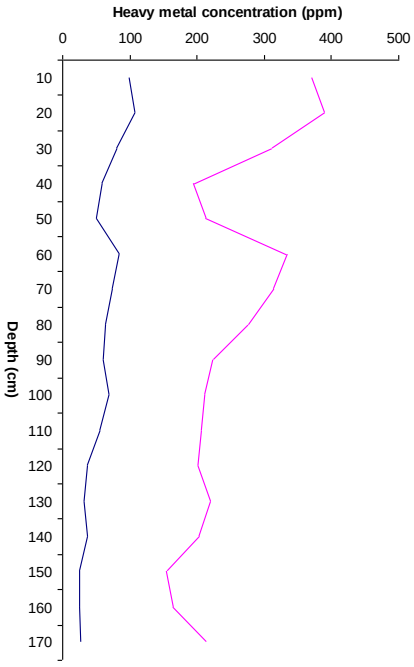

Figure 5. Metal concentration profile

Transect 1 coring 5

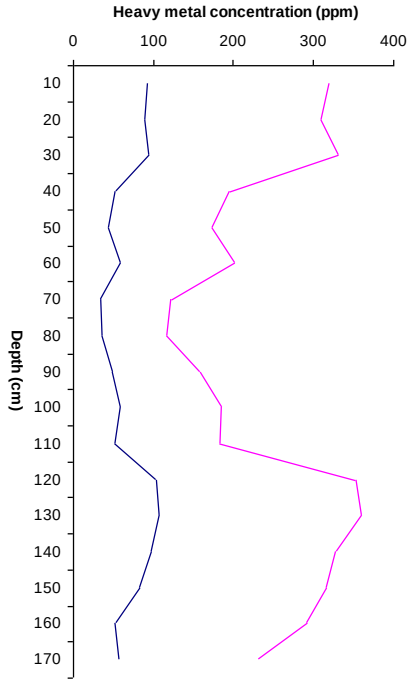

Figure 6. Soil concentration profile

Transect 1 coring 6

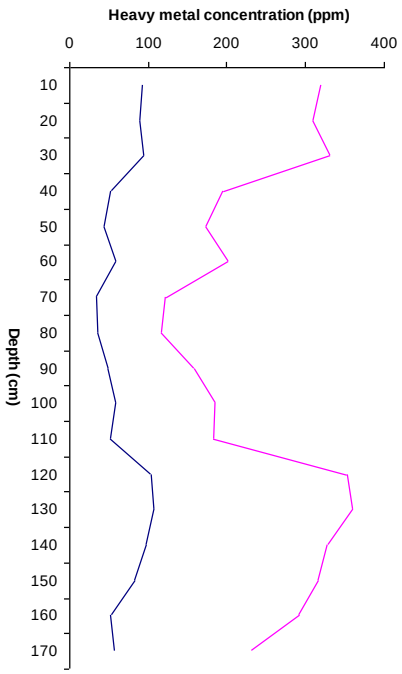

Figure 7. Metal concentration profile

Transect 1 coring 7

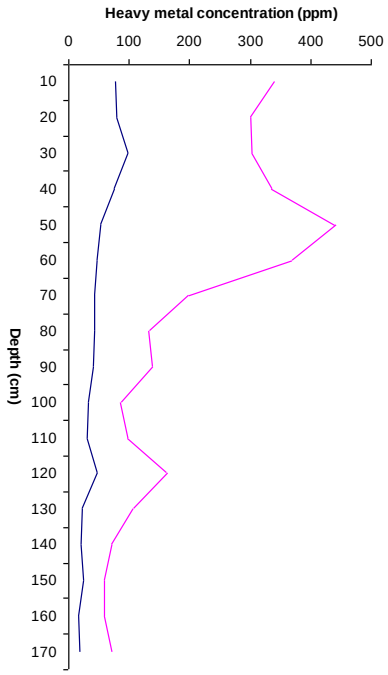

Figure 8. Metal concentration profile

Transect 1 coring 8

Transect 2

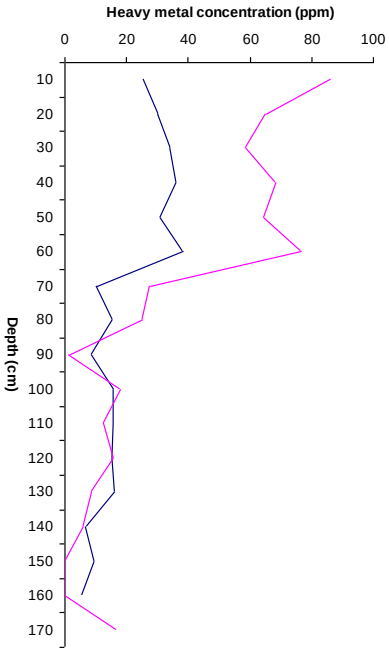

Figure 9. Metal concentration profile

Transect 2 coring 1

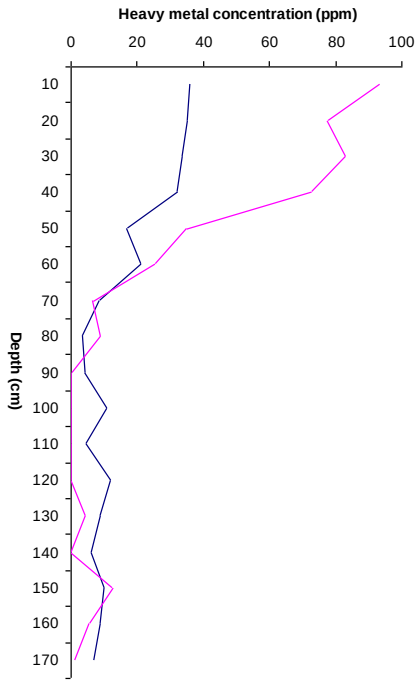

Figure 10. Metal concentration profile

Transect 2 coring 2

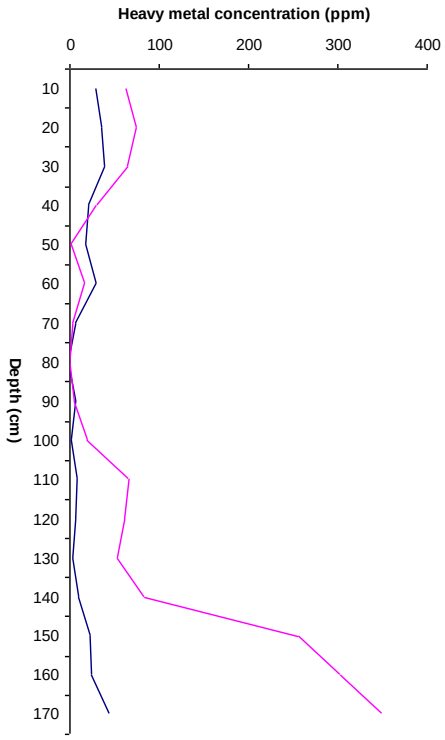

Figure 11. Metal concentration profile

Transect 2 coring 3

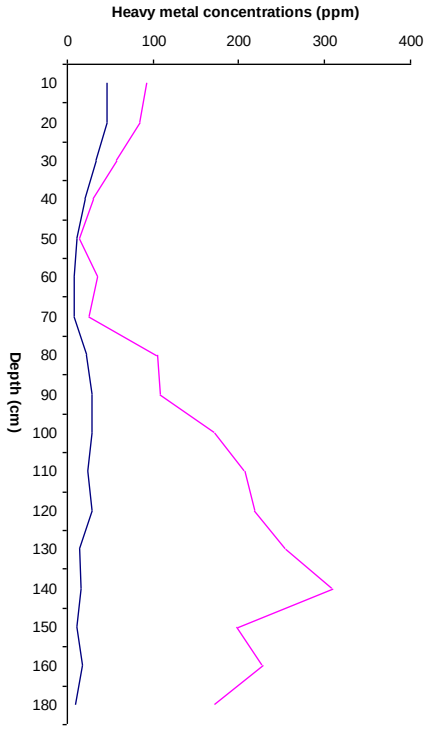

Figure 12. Metal concentration profile

Transect 2 coring 4

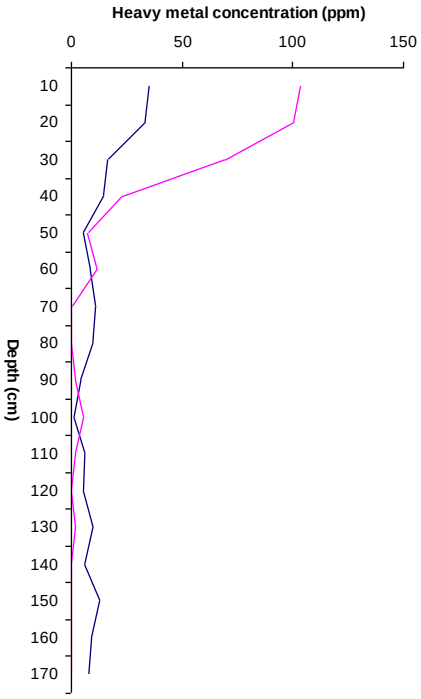

Figure 13. Metal concentration profile

Transect 2 coring 5

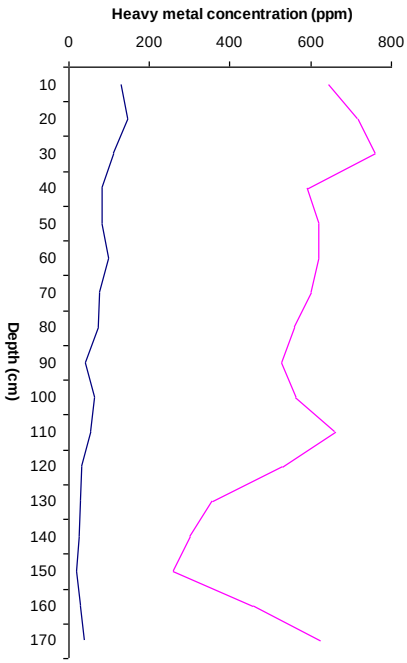

Figure 14. Metal concentration profile

Transect 2 coring 6

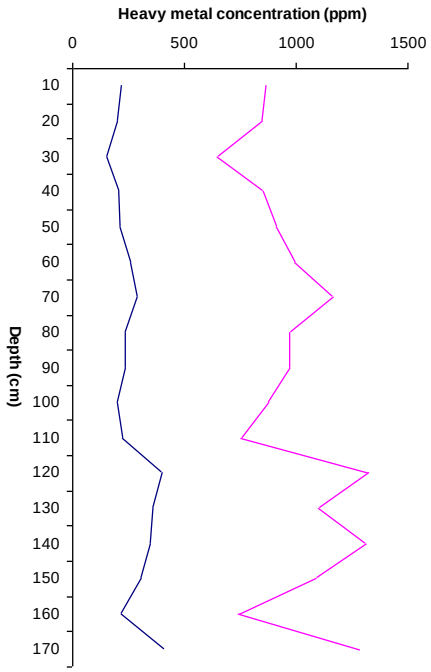

Figure 15. Metal concentration profile

Transect 2 coring 7

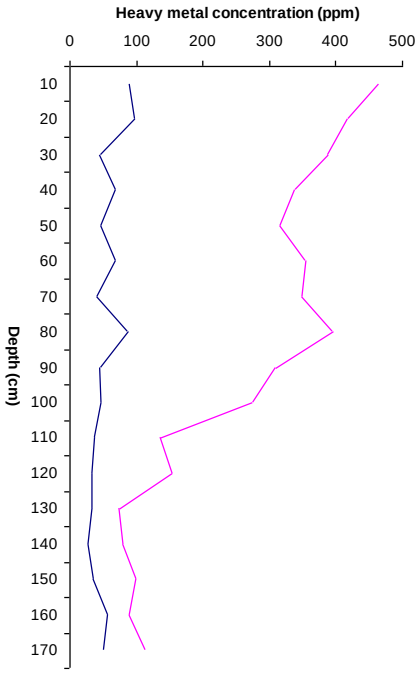

Figure 16. Metal concentration profile

Transect 2 coring 8

Transect 3

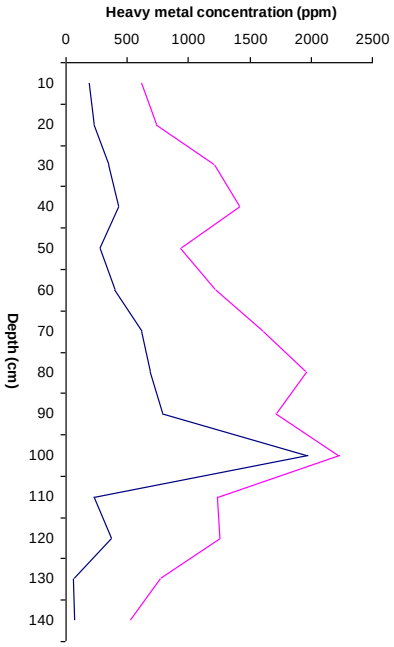

Figure 17. Metal concentration profile

Transect 3 coring 1

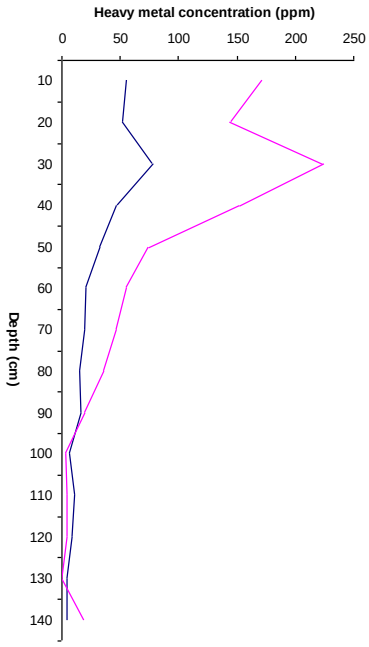

Figure 18. Metal concentration profile

Transect 3 coring 2

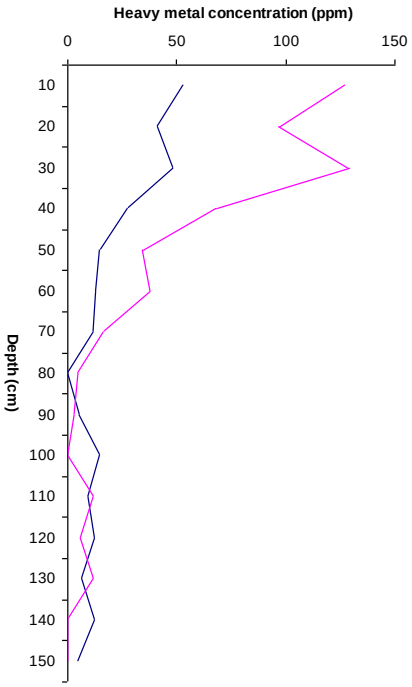

Figure 19. Metal concentration profile

Transect 3 coring 3

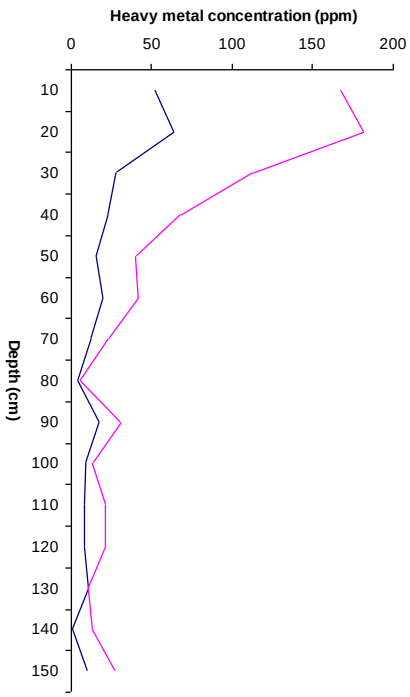

Figure 20. Metal concentration profile

Transect 3 coring 4

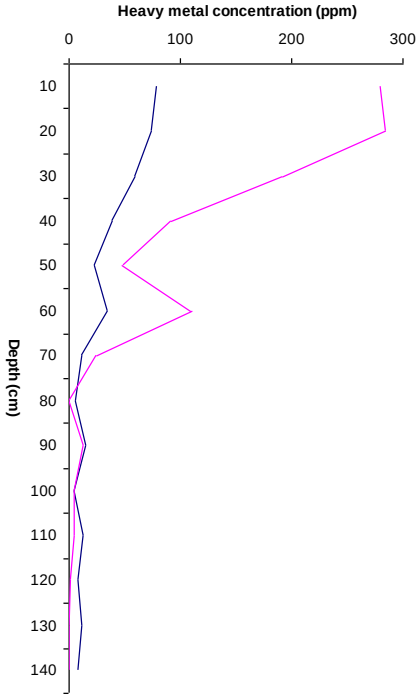

Figure 21. Metal concentration profile

Transect 3 coring 5

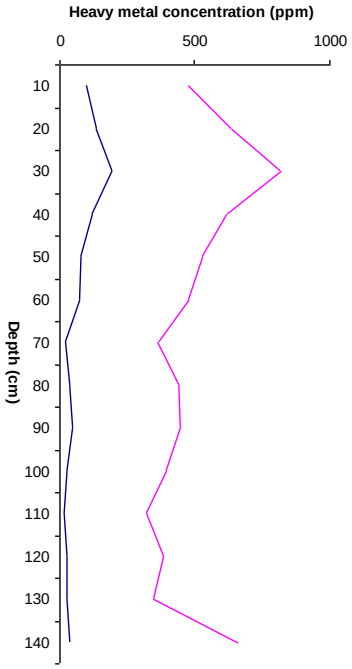

Figure 22. Metal concentration profile

Transect 3 coring 6

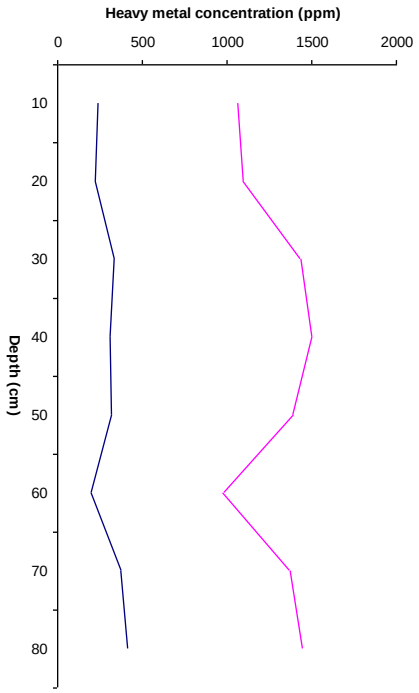

Figure 23. Metal concentration profile

Transect 3 coring 7

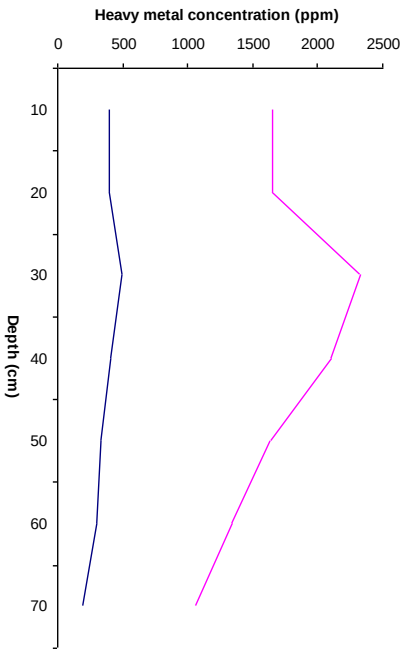

Figure 24. Metal concentration profile

Transect 3 coring 8

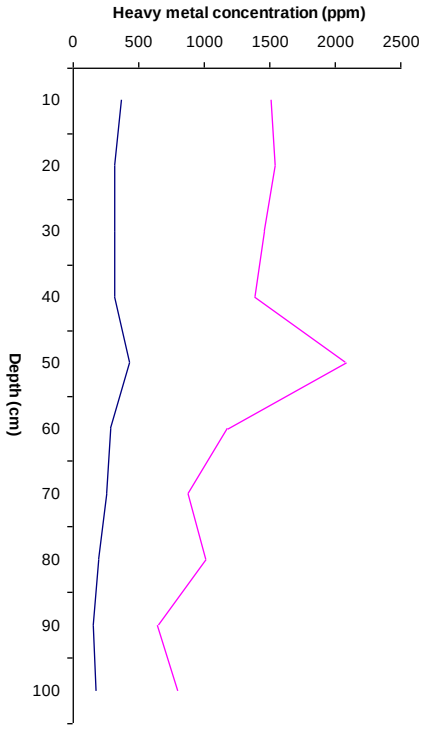

Figure 25. Metal concentration profile

Transect 3 coring 9

Transect 4

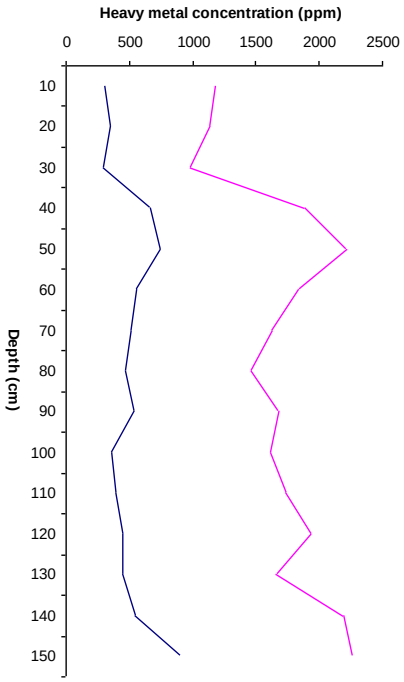

Figure 26. Metal concentration profile

Transect 4 coring 1

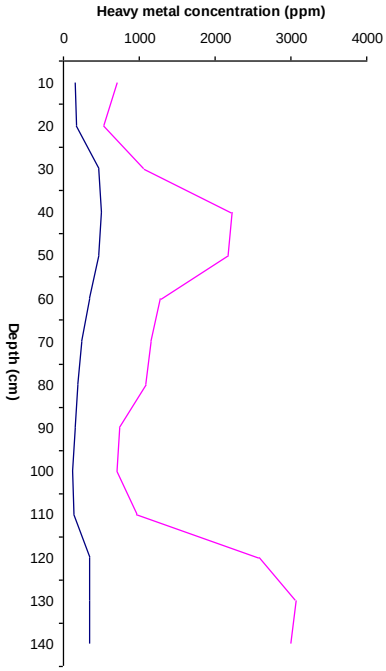

Figure 27. Metal concentration profile

Transect 4 coring 2

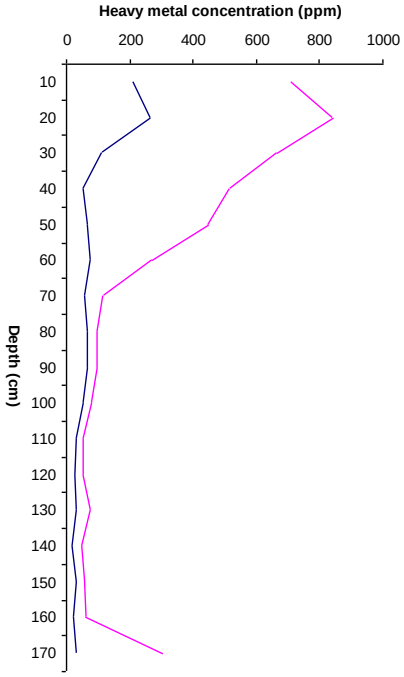

Figure 28. Metal concentration profile

Transect 4 coring 3

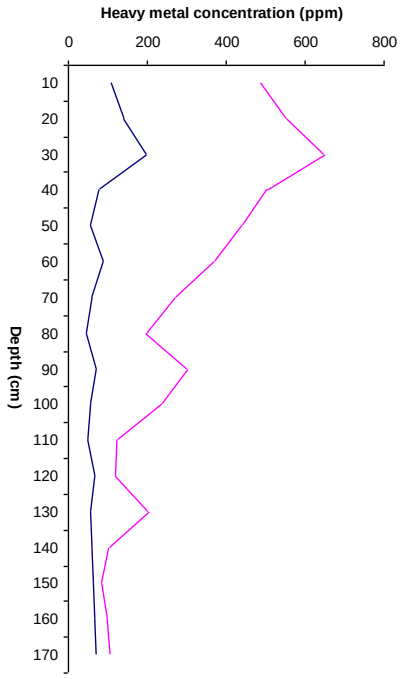

Figure 29. Metal concentration profile

Transect 4 coring 4

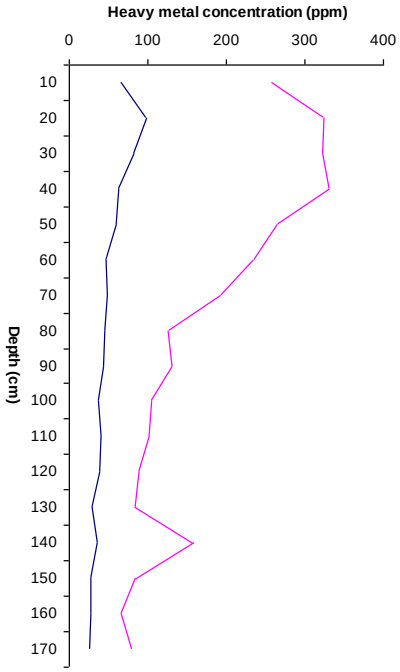

Figure 30. Metal concentration profile

Transect 4 coring 5

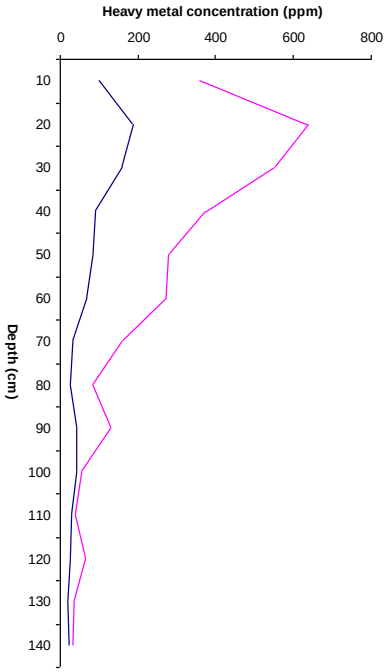

Figure 31. Metal concentration profile

Transect 4 coring 6

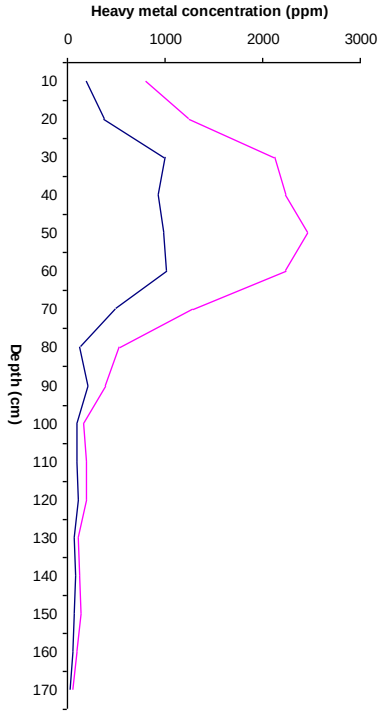

Figure 32. Metal concentration profile

Transect 4 coring 7

Transect 6

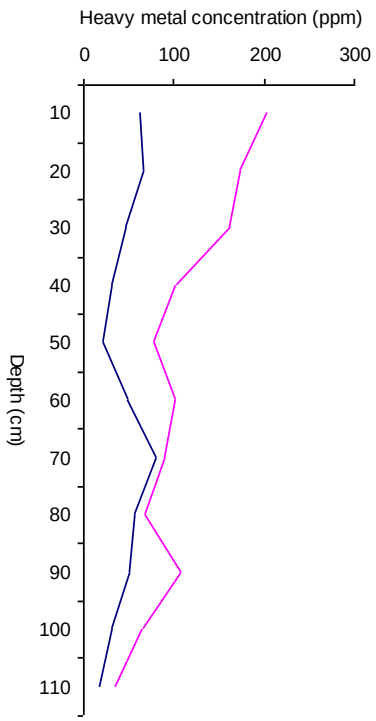

Figure 33. Metal concentration profile

Transect 6 coring 1

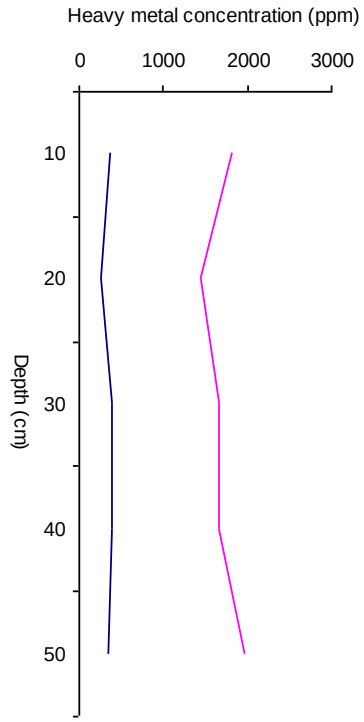

Figure 34.Metal concentration profile

Transect 6 coring 2

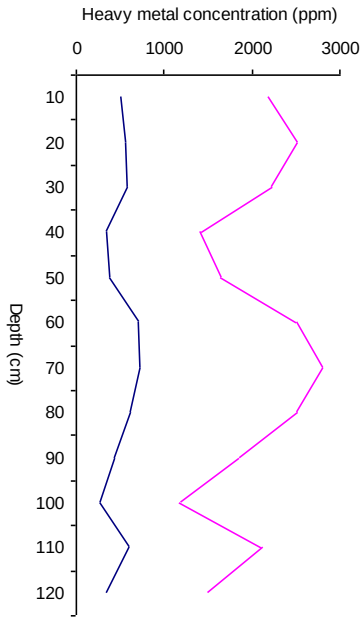

Figure 35. Metal concentration profile

Transect 6 coring 3

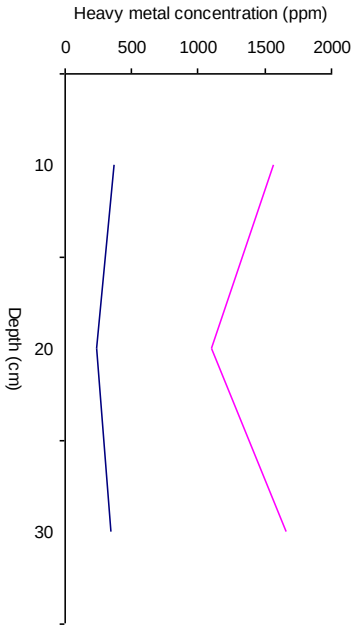

Figure 36. Metal concentration profile

Transect 6 coring 4

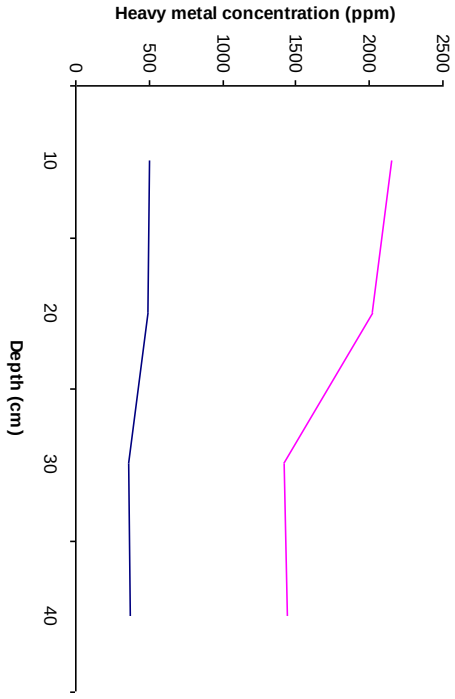

Figure 37. Metal concentration profile

Transect 6 coring 5

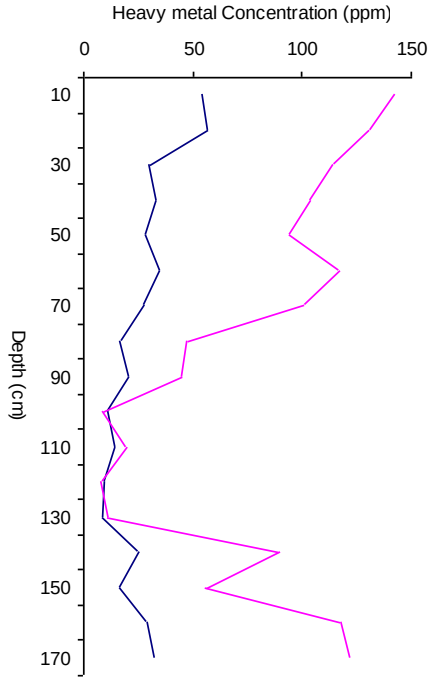

Figure 38. Metal concentration profile

Transect 6 coring 6

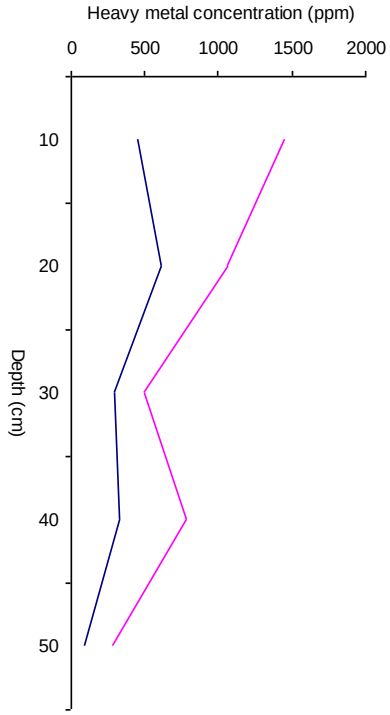

Figure 39. Metal concentration profile

Transect 6 coring 7

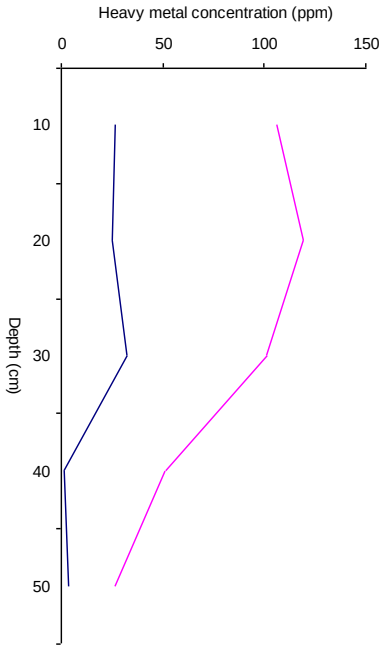

Figure 40. Metal concentration profile

Transect 6 coring 8

Transect 7

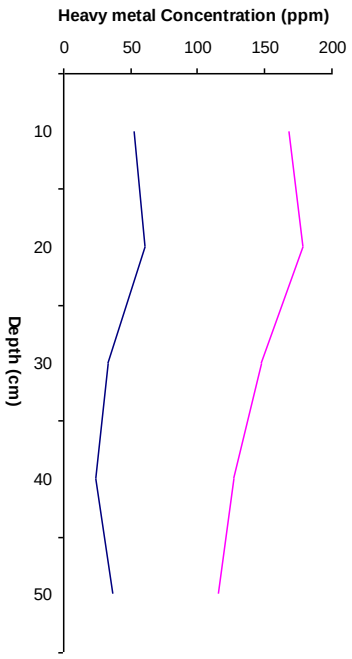

Figure 41. Metal concentration profile

Transect 7 coring 1

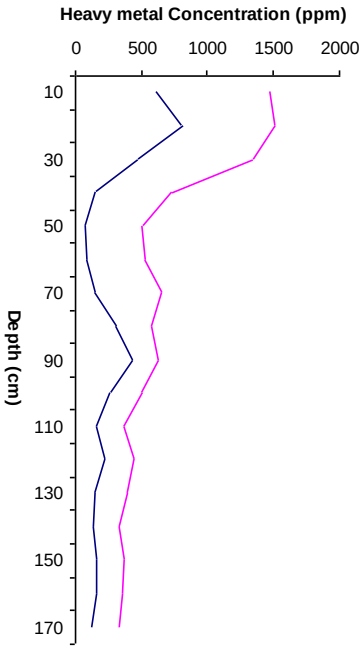

Figure 42. Metal concentration profile

Transect 7 coring 2

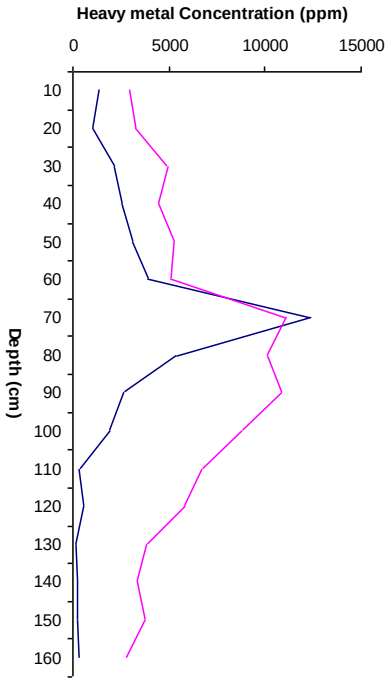

Figure 43. Metal concentration profile

Transect 7 coring 3

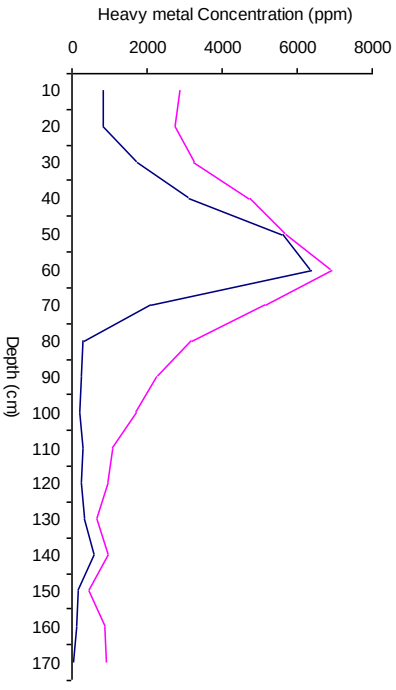

Figure 44. Metal concentration profile

Transect 7 coring 4

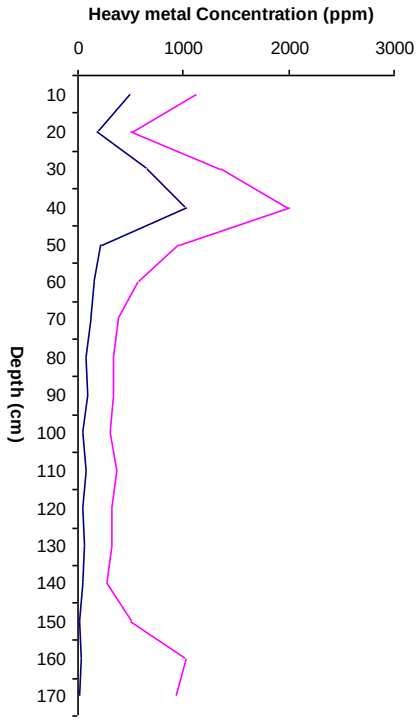

Figure 45. Metal concentration profile

Transect 7 coring 5

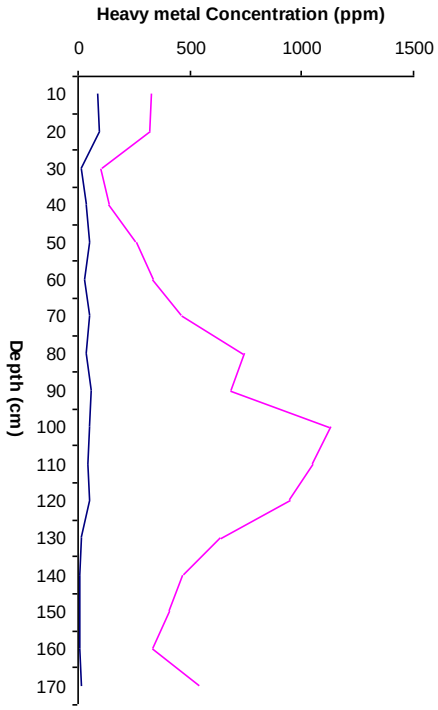

Figure 46. Metal concentration profile

Transect 7 coring 6

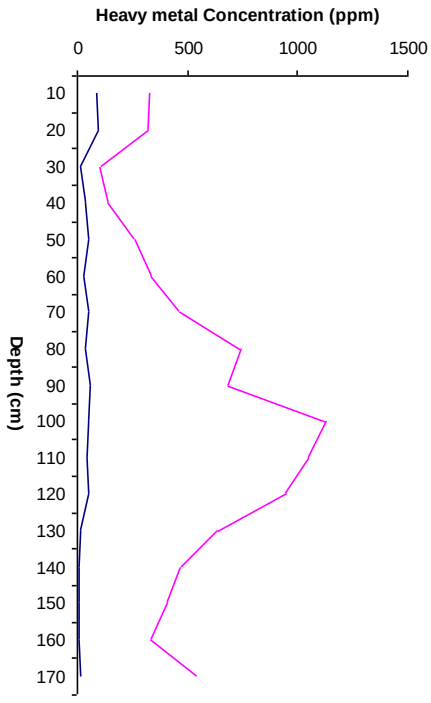

Figure 47. Metal concentration profile

Transect 7 coring 7

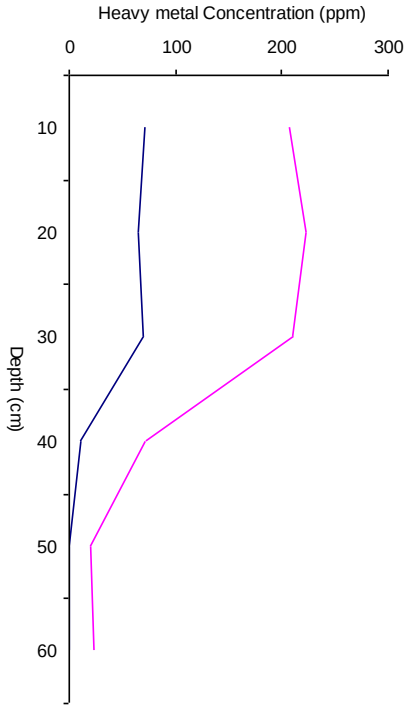

Figure 48. Metal concentration profile

Transect 7 coring 8

Transect 8

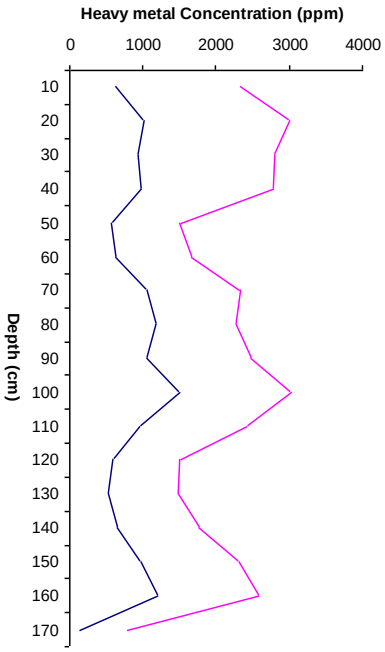

Figure 49. Metal concentration profile

Transect 8 coring 1

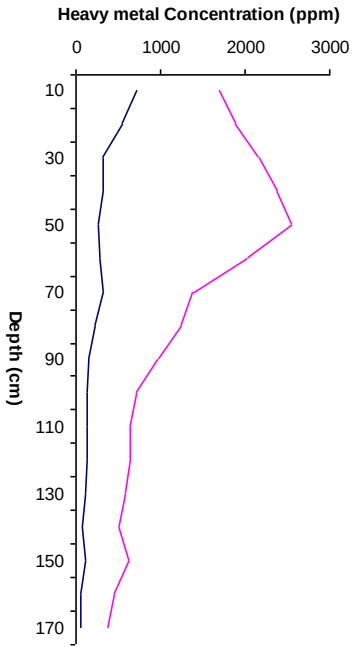

Figure 50. Metal concentration profile

Transect 8 coring 2

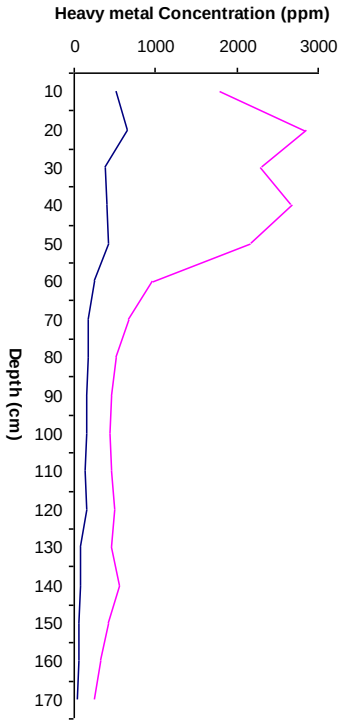

Figure 51. Metal concentration profile

Transect 8 coring 3

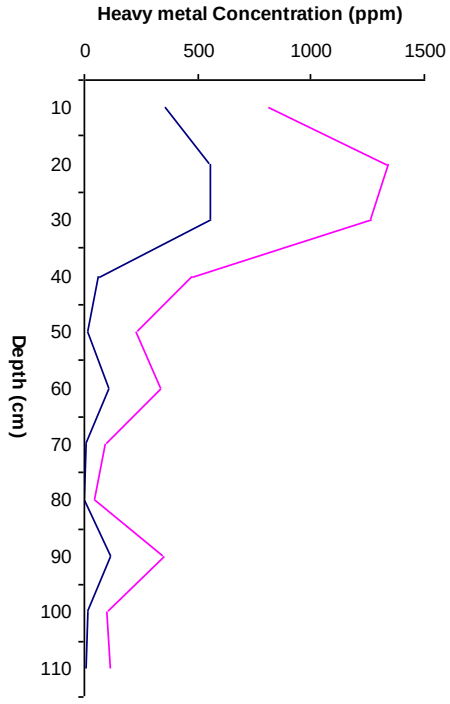

Figure 52. Metal concentration profile

Transect 8 coring 4

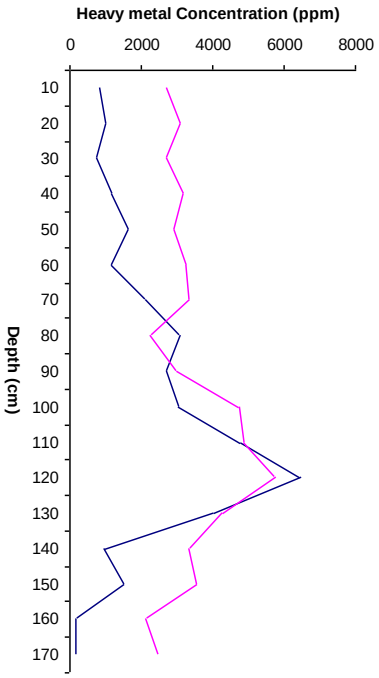

Figure 53. Metal concentration profile

Transect 8 coring 5

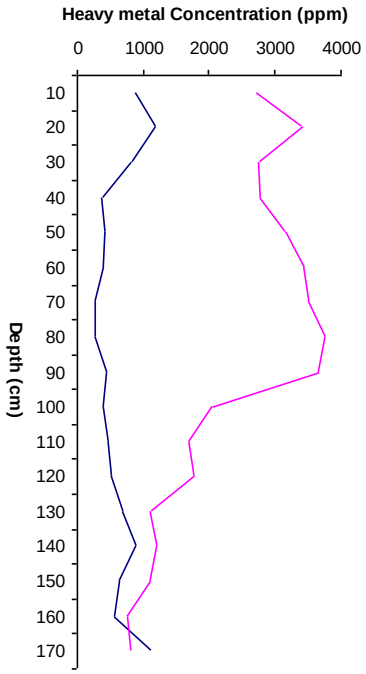

Figure 54. Metal concentration profile

Transect 8 coring 6

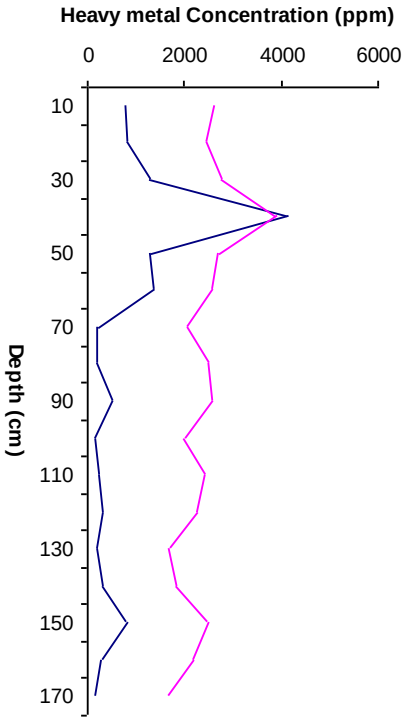

Figure 55. Metal concentration profile

Transect 8 coring 7

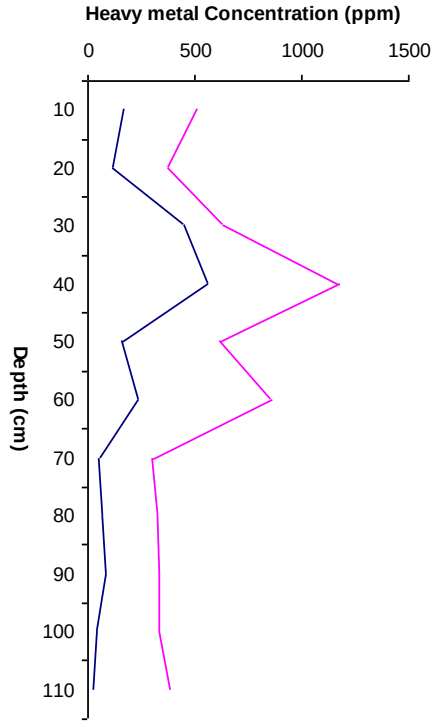

Figure 56. Metal concentration profile

Transect 8 coring 8

Transect 9

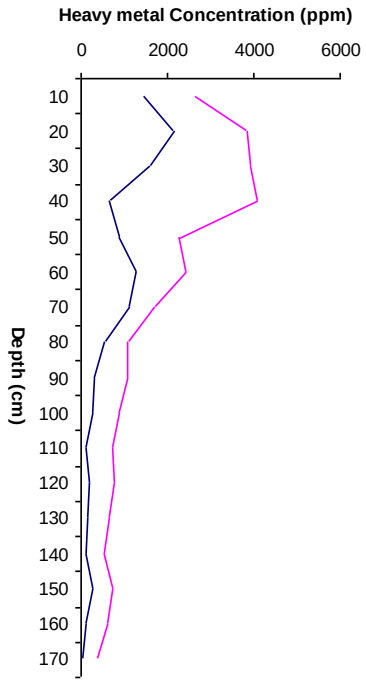

Figure 57. Metal concentration profile

Transect 9 coring 1

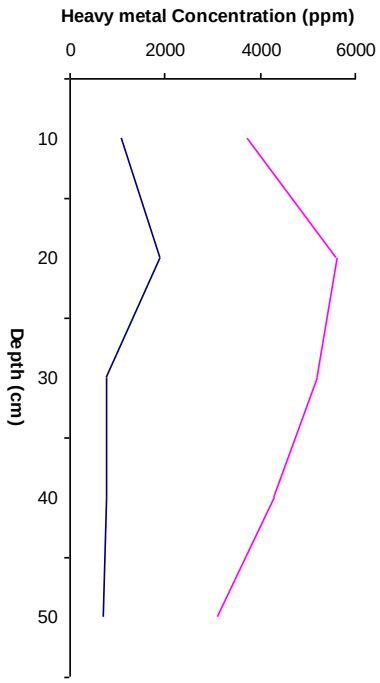

Figure 58. Metal concentration profile

Transect 9 coring 2

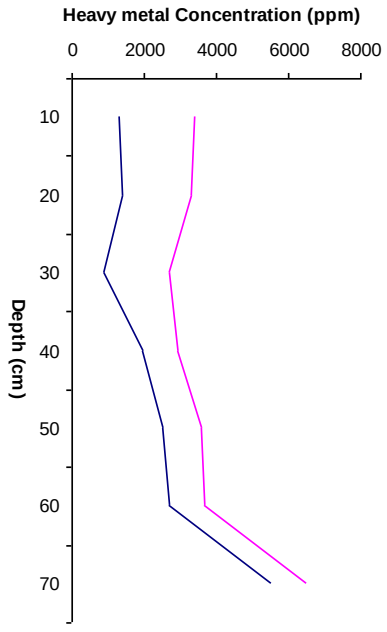

Figure 59. Metal concentration profile

Transect 9 coring 3

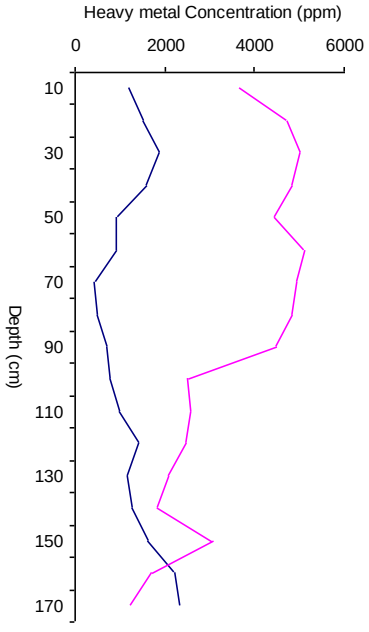

Figure 60. Metal concentration profile

Transect 9 coring 4

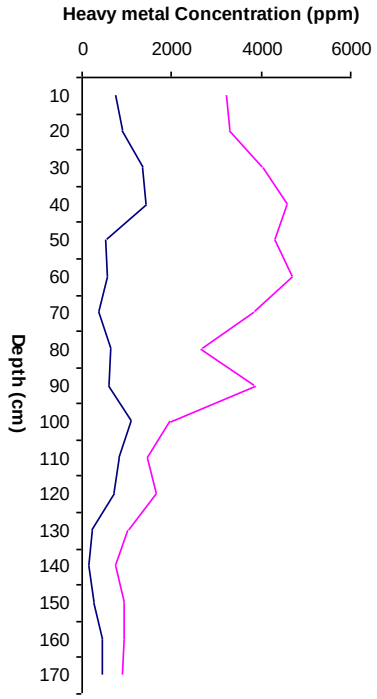

Figure 61. Metal concentration profile

Transect 9 coring 5

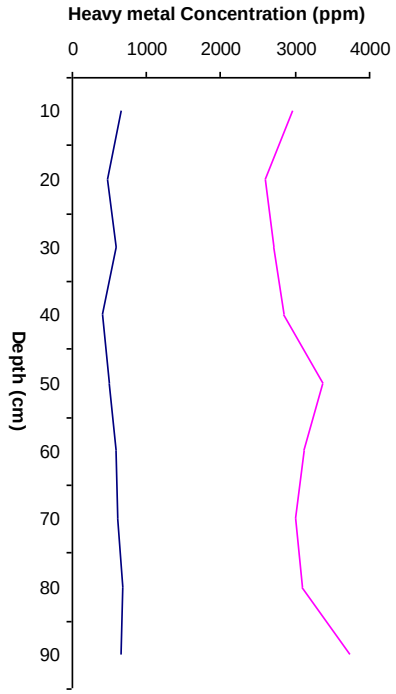

Figure 62. Metal concentration profile

Transect 9 coring 6

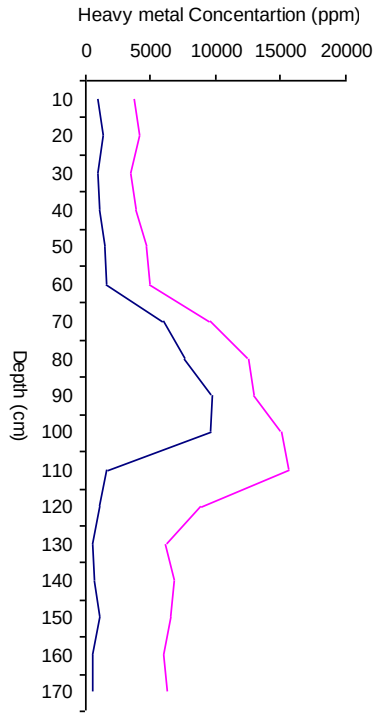

Figure 63. Metal concentration profile

Transect 9 coring 7

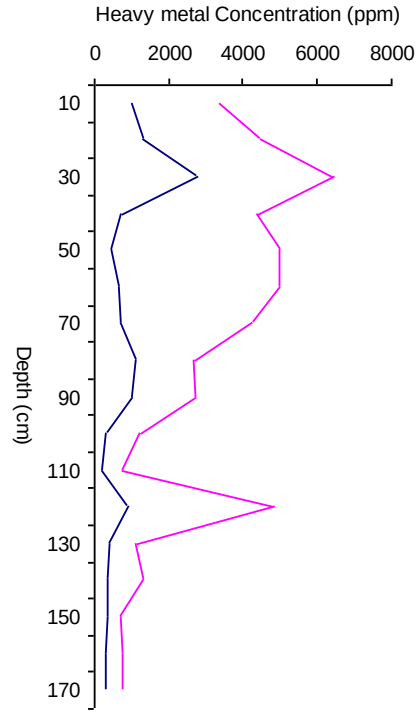

Figure 64. Metal concentration profile

Transect 9 coring 8

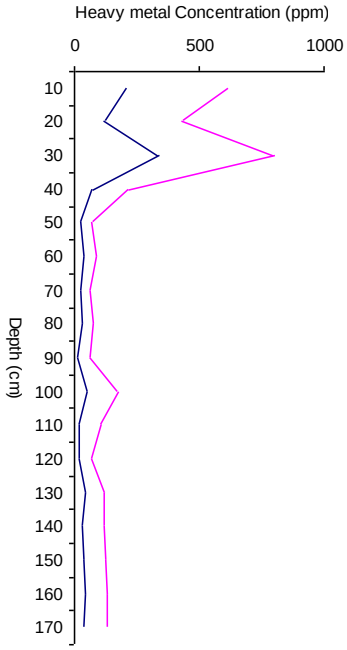

Figure 65. Metal concentration profile

Transect 9 coring 9

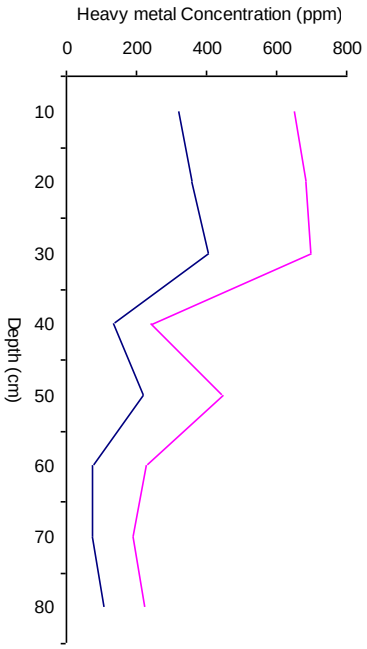

Figure 66. Metal concentration profile

Transect 9 coring 10

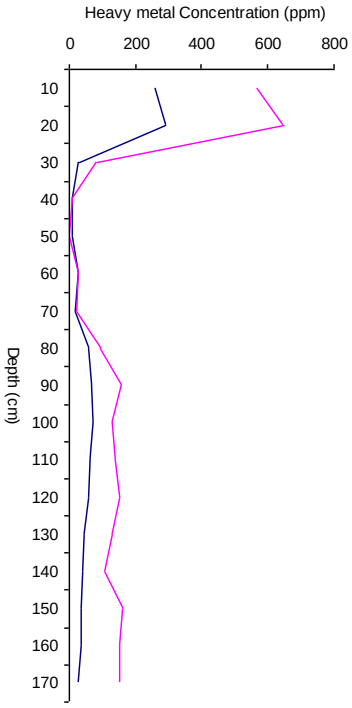

Figure 67. Metal concentration profile

Transect 9 coring 11